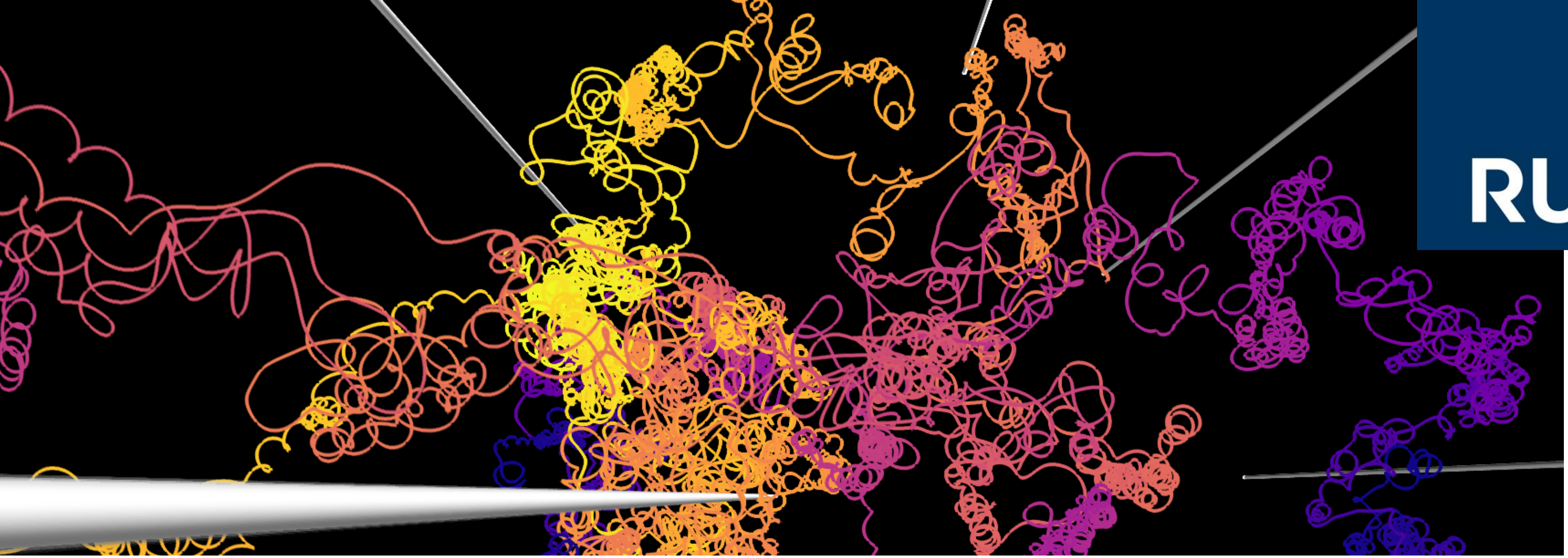

RUHR-UNIVERSITÄT BOCHUM

CRPropa 3.1

Propagation of cosmic rays in the transition region

CRA 2017, Guadalajara /Bochum

FAKULTÄT für Physik und Astronomie
Lehrstuhl für Theoretische Physik IV
Plasma Astroteilchen
Lukas Merten

Introduction

Lukas Merten

PhD student

Loves skyping

Collaboration

Ruhr-Universität Bochum

- Lukas Merten
- Julia Tjus
- Björn Eichmann
- Horst Fichtner

University of Hamburg

- Günter Sigl
- Andrej Dundovic

RWTH Aachen

- Daniel Kümpel
- Gero Müller
- David Walz

University of Wisconsin-Madison

- Ellen Zweibel
- Chad Bustard

Contents

1 CRPropa

2 Anisotropic Diffusion

- Stochastic Differential Equations

3 Galactic Propagation

- The coherent component of the JF12 field

4 Galactic Termination Shock

- Possible Source between ‚knee' and ‚ankle'?!

5 Summary / Outlook

1 CRPropa

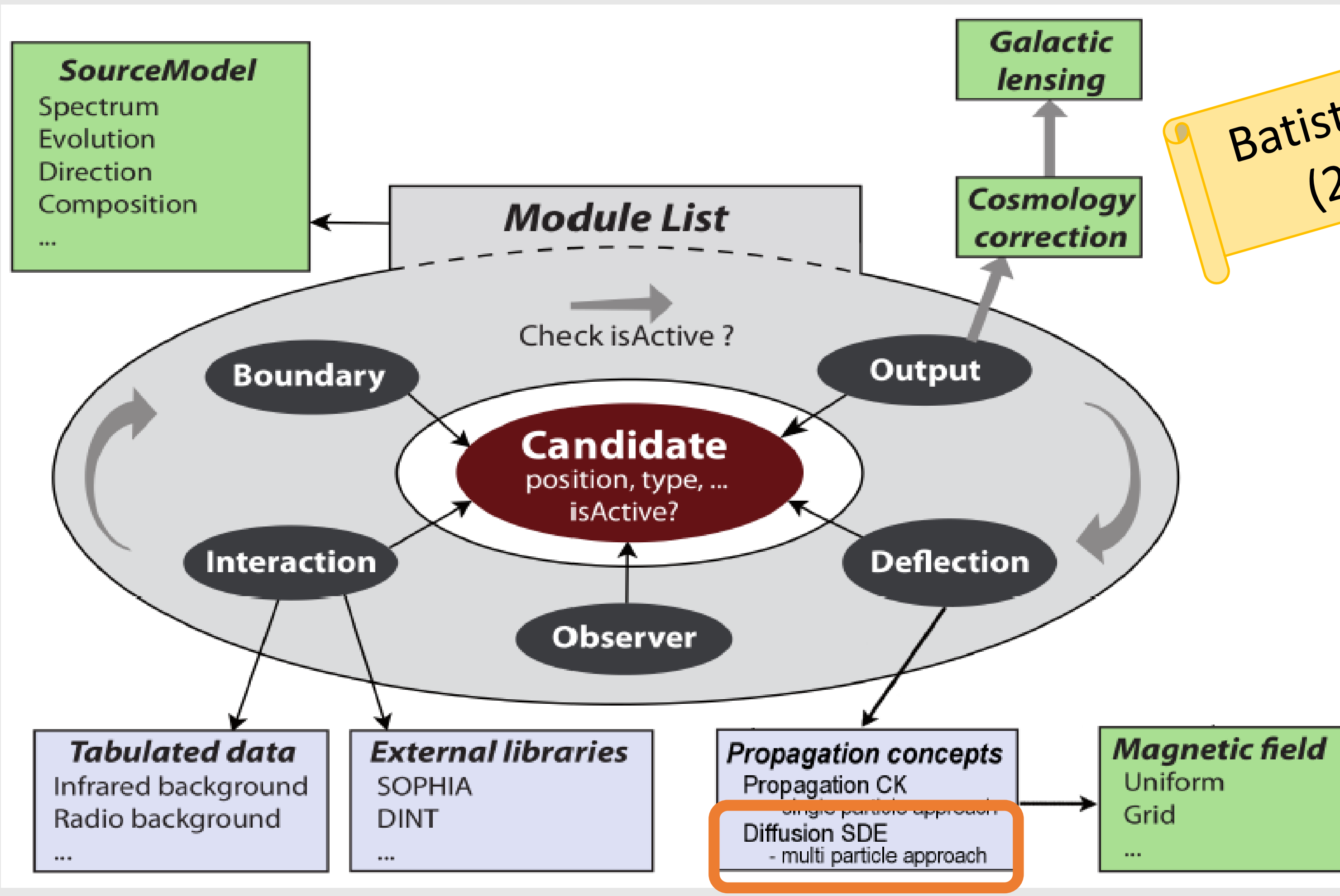

Batista et al. (2016)

Fig 1. The modular structure makes it easy to extend CRPropa 3.

2 Propagation Models

Singleparticle picture

- Solving the equation of motion
- Backtracking and Reweighting of results is possible

Numerics

Multiparticle picture

- Solving the transport equation
- Collective behavior, e.g. advection and diffusion is easy to implement

Physics

Stochastic Differential Equations

2 Parker Transport Equation

Spatial Diffusion

Adiabatic cooling

$$\frac{\partial n}{\partial t} + \vec{u} \cdot \nabla n = \nabla \cdot (\hat{\kappa} \nabla n) + \frac{1}{p^2}\frac{\partial}{\partial p}\left(p^2 \kappa_{pp} \frac{\partial n}{\partial p}\right) + \frac{1}{3}(\nabla \cdot \vec{u}) \frac{\partial n}{\partial \ln p} + S(\vec{x}, p, t)$$

Advection

Momentum Diffusion

Sources

2 Spatial Diffusion and Advection

$$\frac{\partial n}{\partial t} + \vec{u} \cdot \nabla n = \nabla \cdot (\hat{\kappa} \nabla n) + \frac{1}{3} (\nabla \cdot \vec{u}) \frac{\partial n}{\partial \ln p} + S(\vec{x}, p, t)$$

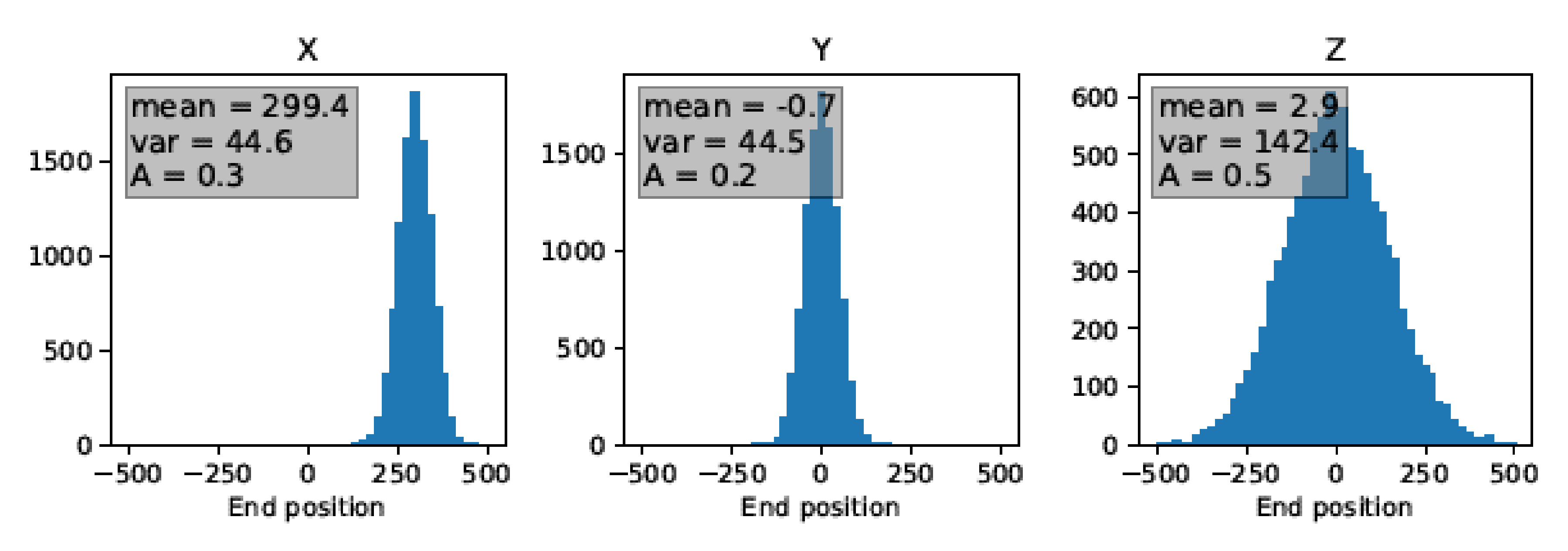

Fig 2. Spatial distribution of 10,000 pseudo-particles positions for anisotropic diffusion and advection.

3 The Laboratory

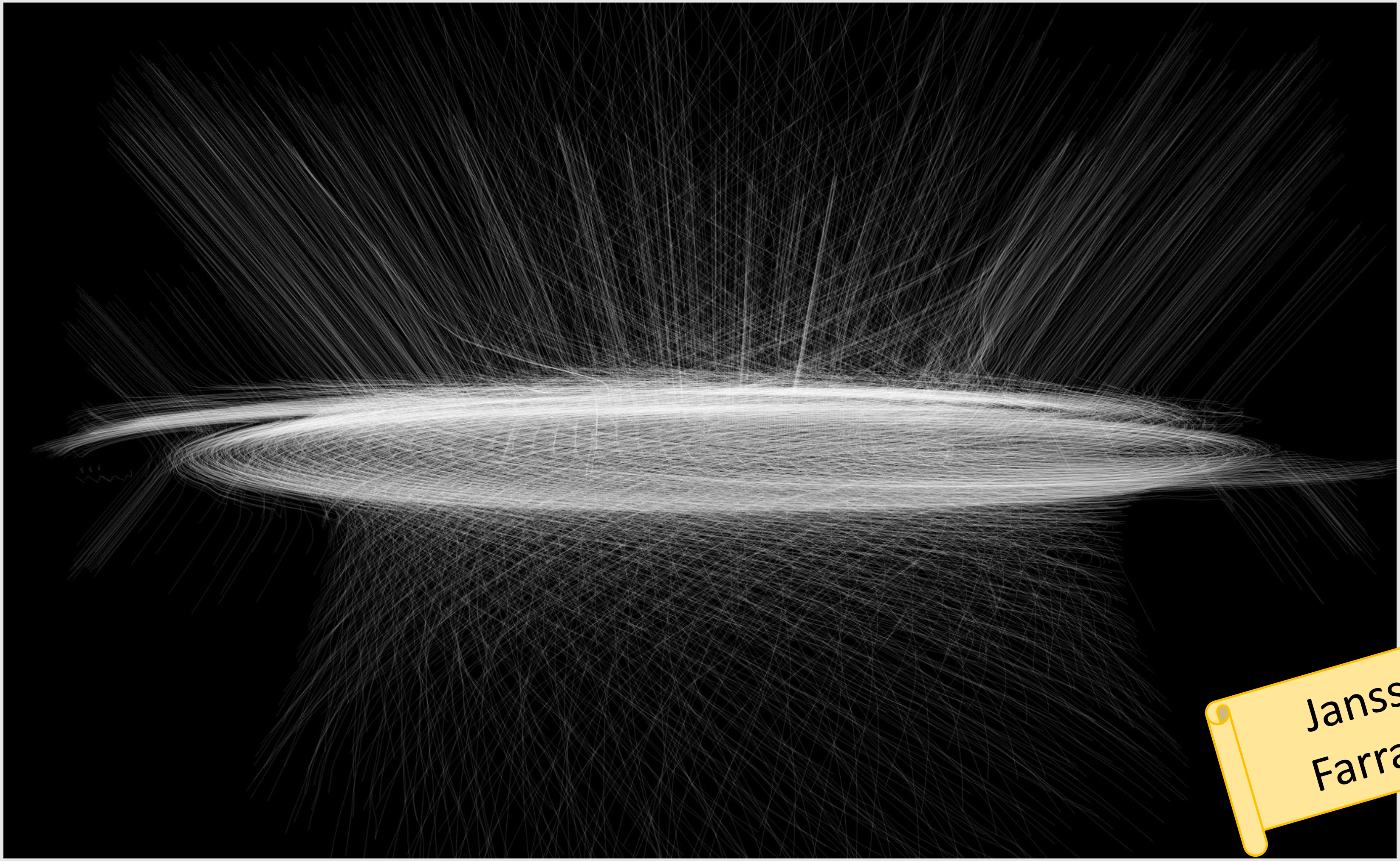

Fig 3. The coherent, regular component of the Galactic Magnetic field which is used as the background field in our simulations.

3 First applications – Diffusion tensor, $R = 10\text{TV}$

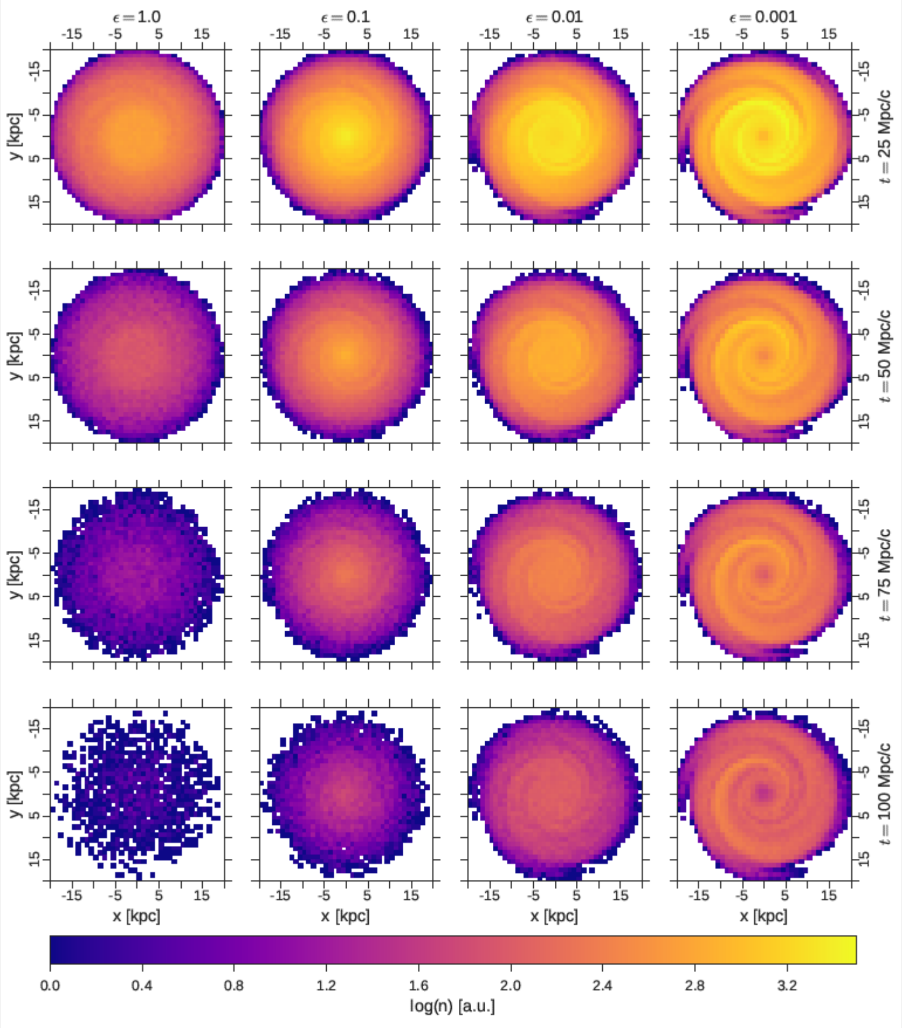

Fig 3: Density inside the Galactic disc.

- Magnetic field structure becomes clearly visible for strong parallel diffusion.
- Highest density at Galactic center for strong perpendicular diffusion
- Differences in loss time become visible.

3 First applications – Diffusion tensor

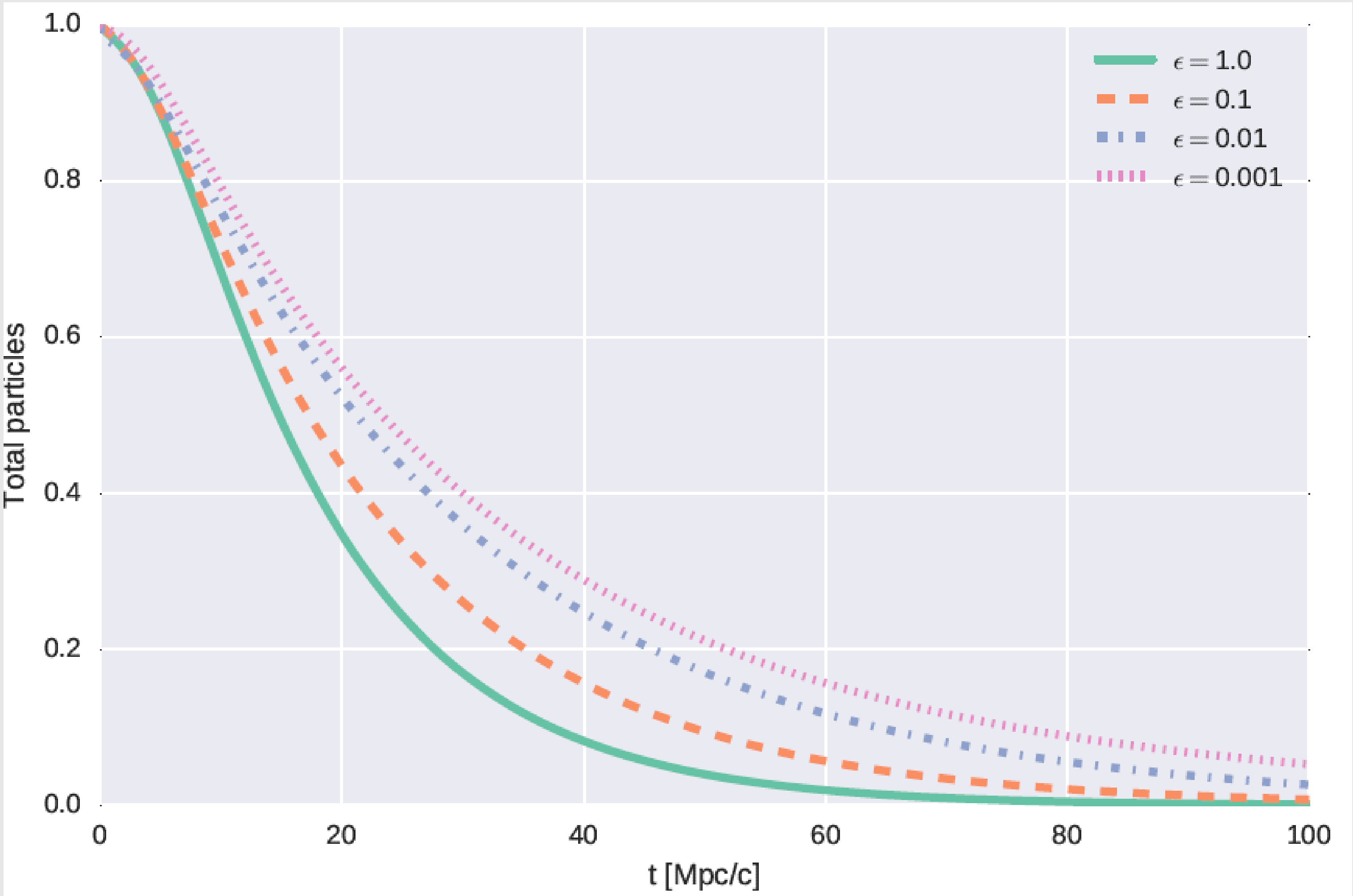

Fig 4: Time Evolution of the total particle number.

3 First applications – Rigidity, $\epsilon = 0.1$

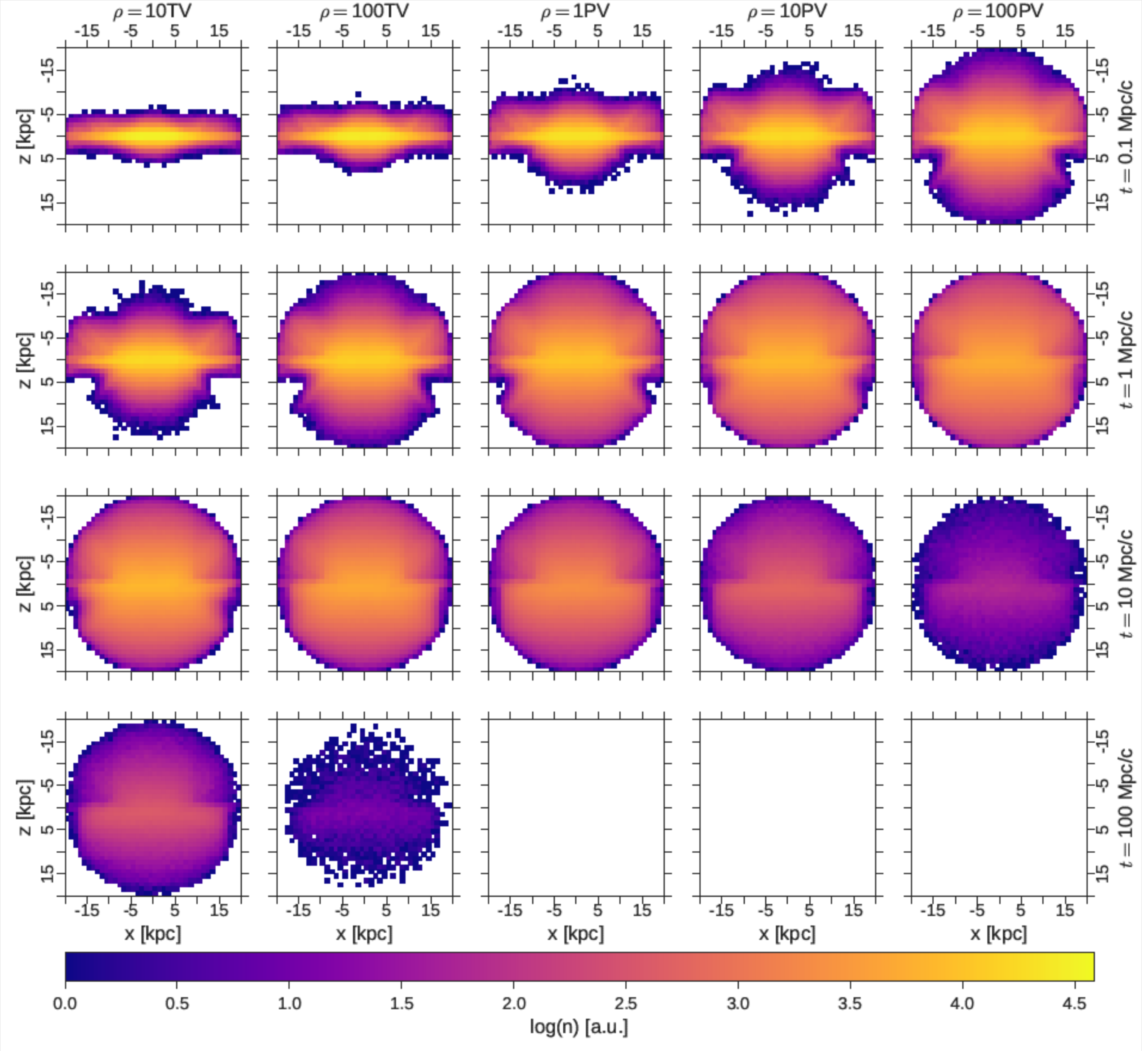

Fig 5: Projected density inside simulation volume.

- Outflow along the magnetic field lines is visible
- Differences in loss time depending on rigidity is huge
- Structures are washed out with time

4 Galactic Termination Shock

Acceleration is possible up to $E = 10^{16} eV$ (see Bustard et al. (2016)).

Isotropic (?) flux in the „knee“ to „ankle“ region.

Possible explanation for the transition region

Can CRs diffuse back to the Galactic disk?

Build a model in CRPropa to find out.

4 Model Sketch

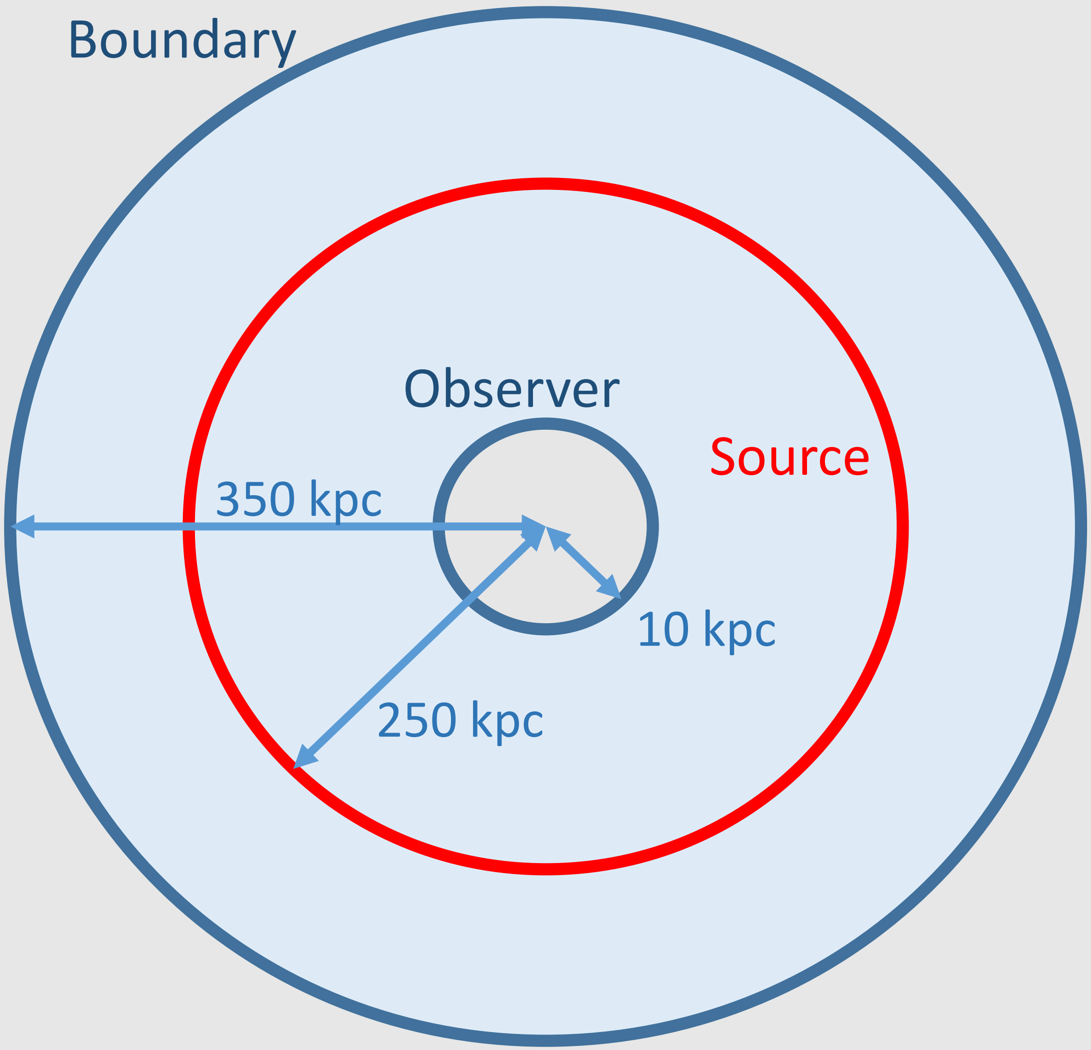

Fig 6: The Galactic termination shock model

Symmetry

- Radial / Archmedean spiral

Diffusion

- D$\propto E^{\delta}$
- $D_0 = 10^{28} \frac{cm^2}{s}$

Advection

- $v_0 = 600 \frac{km}{s}$
- $r_0 = 250\ kpc$

4 Archmedean Spiral

$$\frac{\mathbf{B}}{B_0} = \underbrace{\left[1 - 2S\left(\theta - \frac{\pi}{2}\right)\right]}_{\text{change direction at z=0}} \left(\frac{r_{\mathrm{ref}}^2}{r^2}\mathbf{e}_r - \frac{\Omega r_{\mathrm{ref}}^2 \sin(\theta)}{r V_w}\mathbf{e}_\phi\right)$$

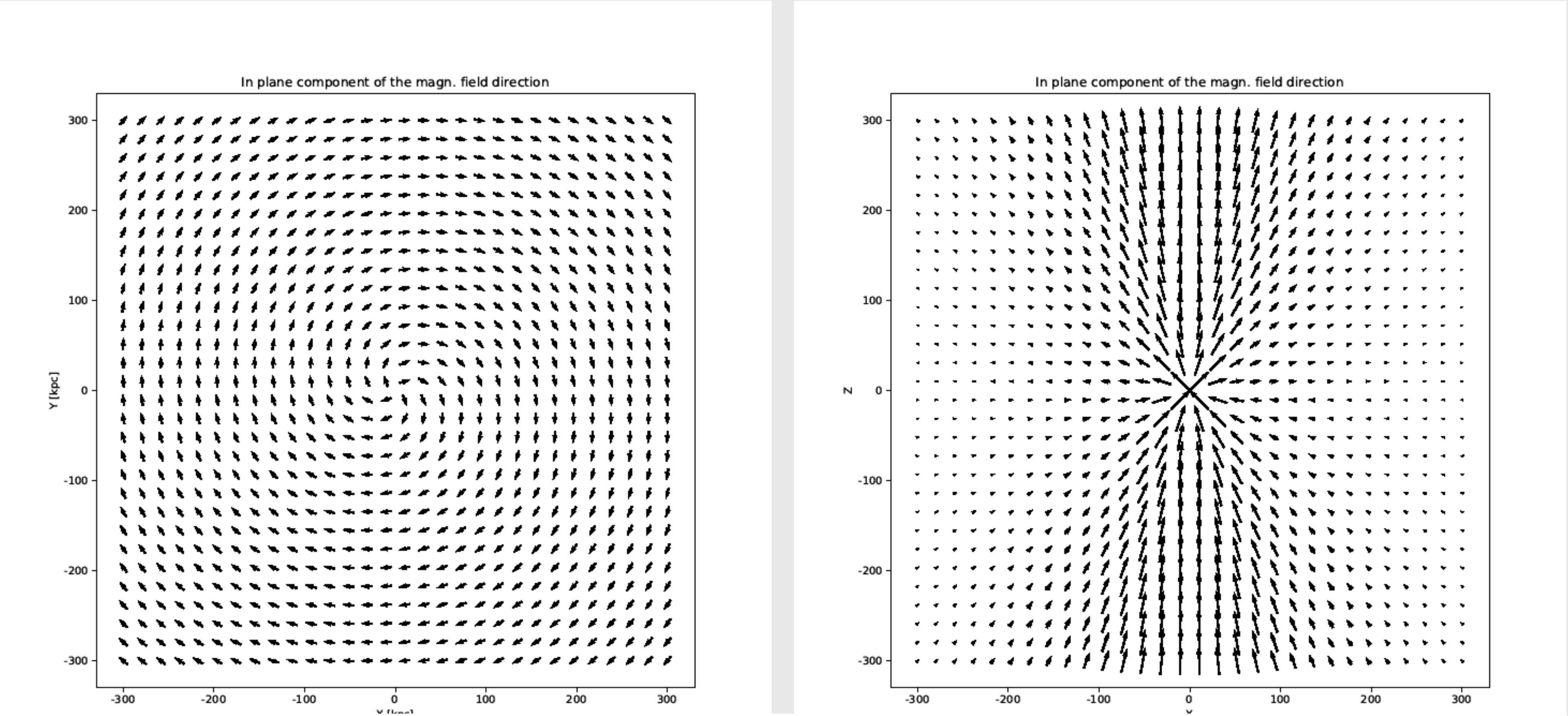

Fig 7: Face- and edge-on view of the background field for the Archmedean spiral model

4 Time Evolution (averaged): $\delta = 0.4$

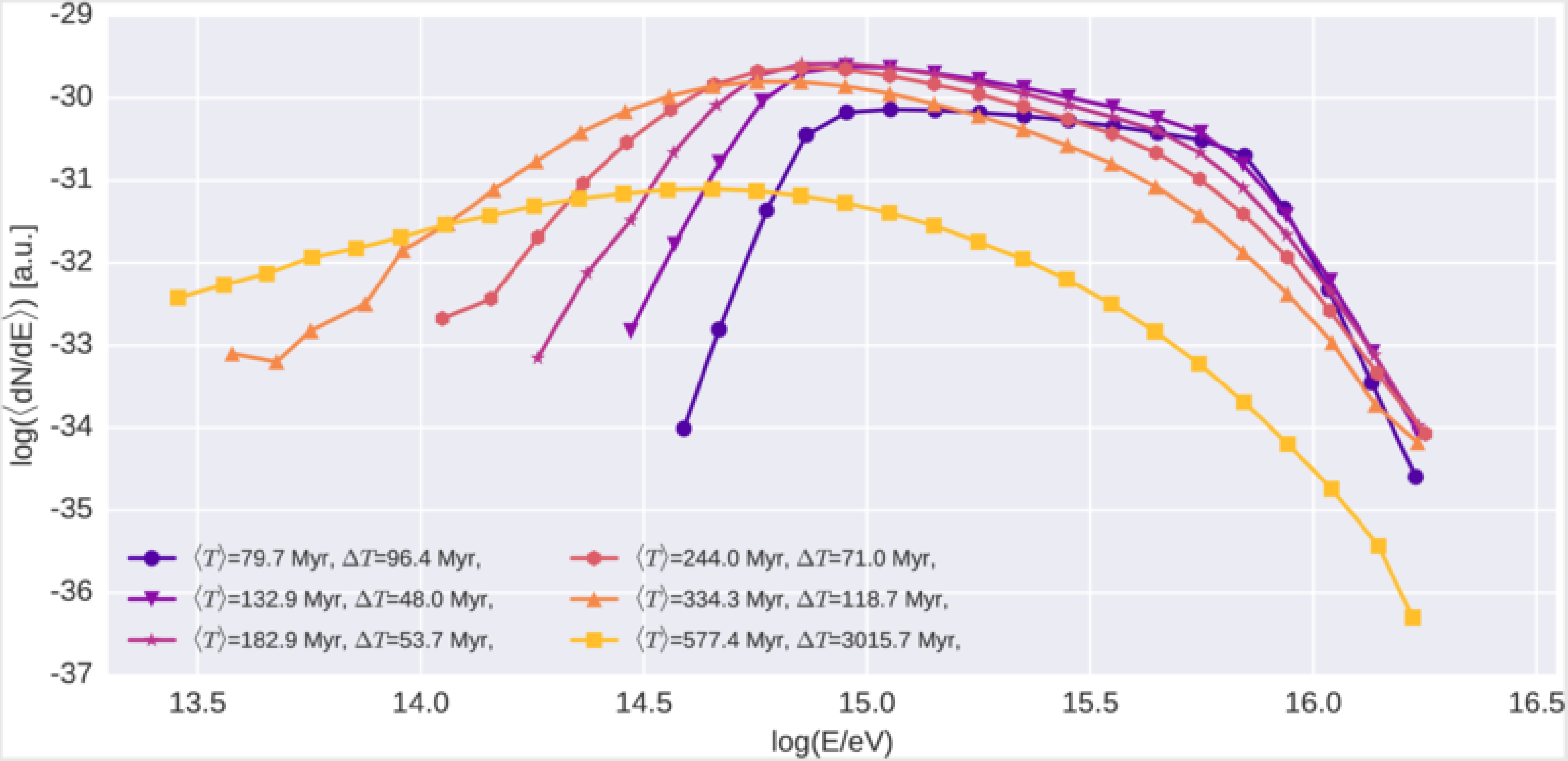

Fig 8: Time Evolution of the observed spectrum for a delta injection in time at the source

4 Green‘s Method

Source is active between t=t_{start}=0 and t=t_{end}=50 Myr

$$S(t) \propto \Theta(t - t_1)\Theta(t - t_0)$$

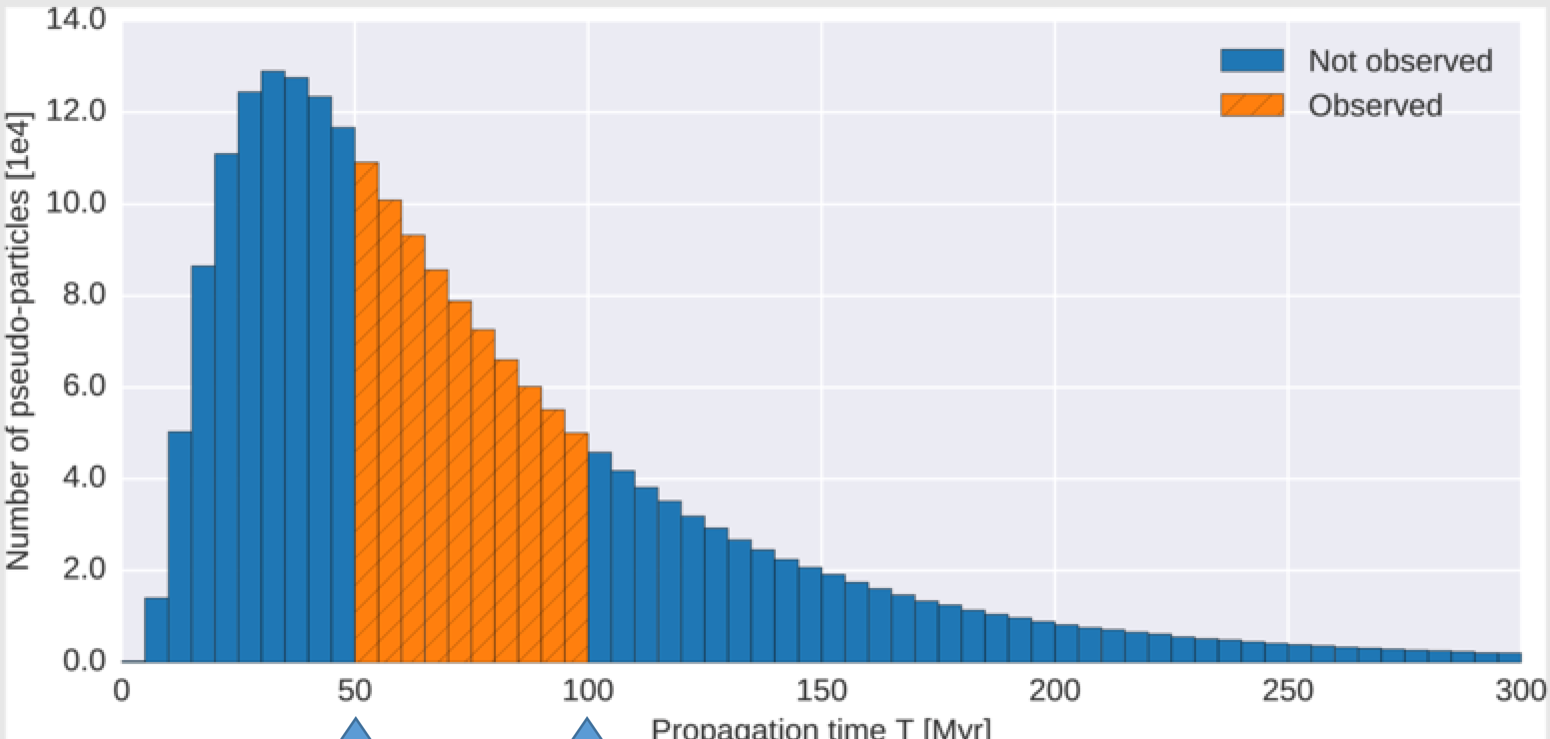

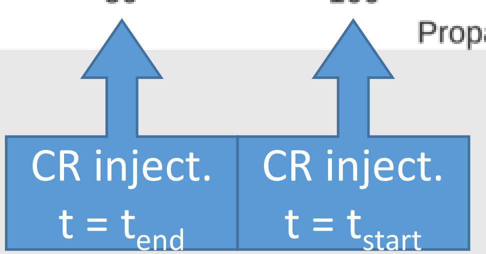

Fig 9: Propagation times. Observed particles for contious emission of $\Delta t = 50$ Myr.

4 Time Evolution - Luminosity

Spherical symmetric | Archmedean spiral

No wind / Wind

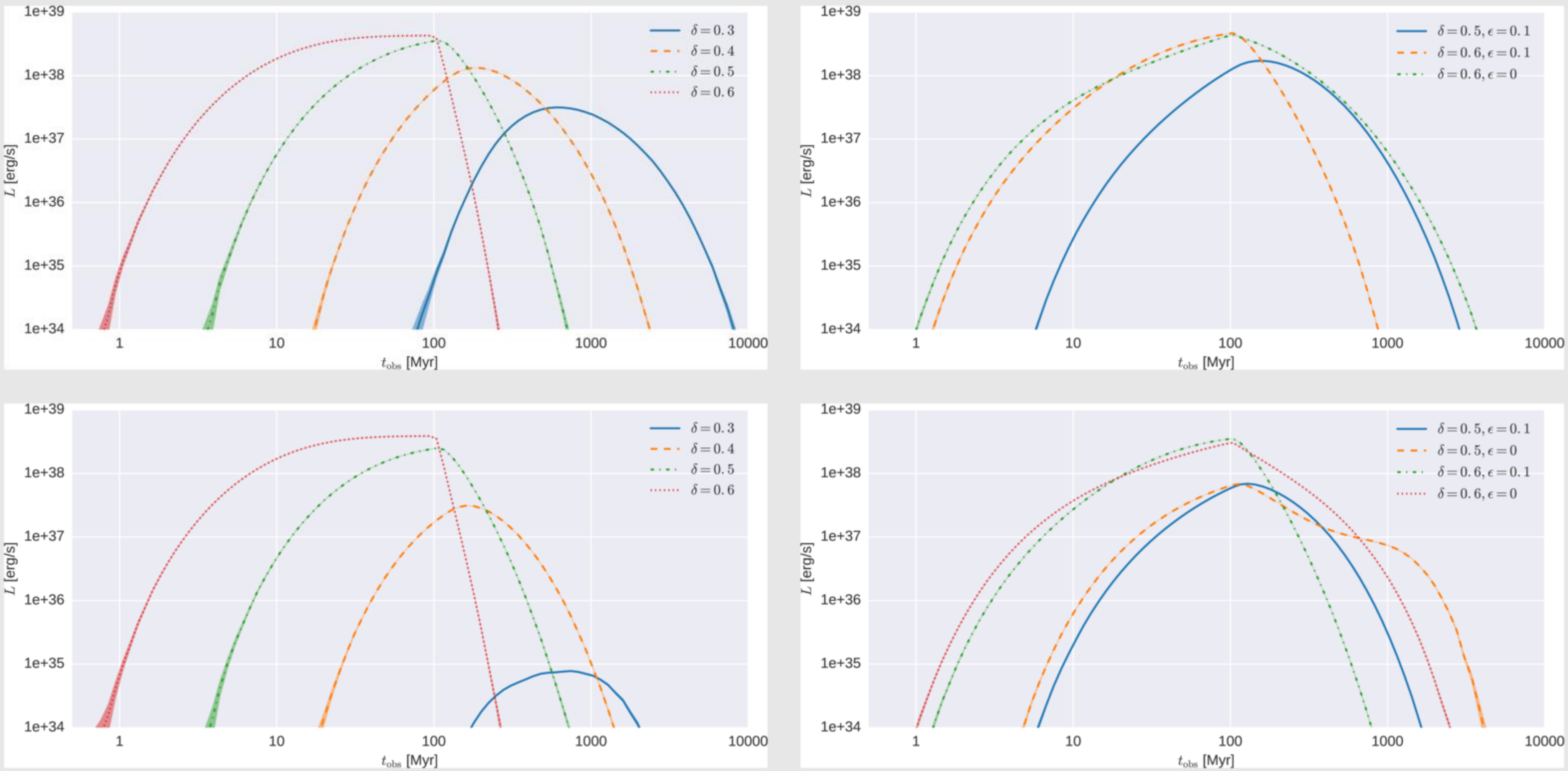

Fig 10: Luminosity evolution for different models.

4 Time Evolution $\Delta t = 100$ Myr; $\delta = 0.5$

Spherical Symmetric – 1 dimensional

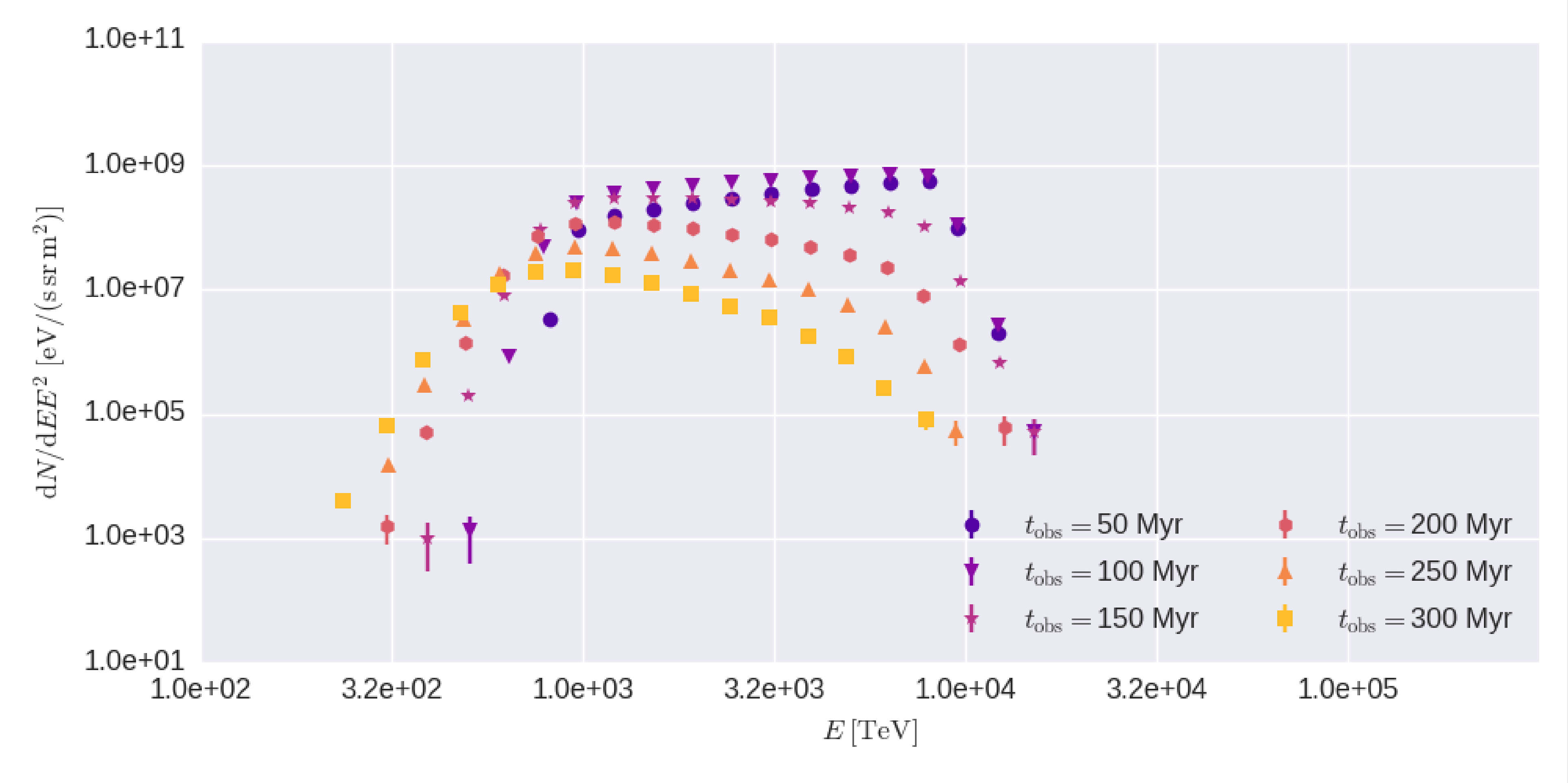

Fig 11: Spectrum including statistical errors.

4 Time Evolution $\Delta t = 100$ Myr; $\delta = 0.5$

Archmedean spiral – 3 dimensional ; $\epsilon = 0.$

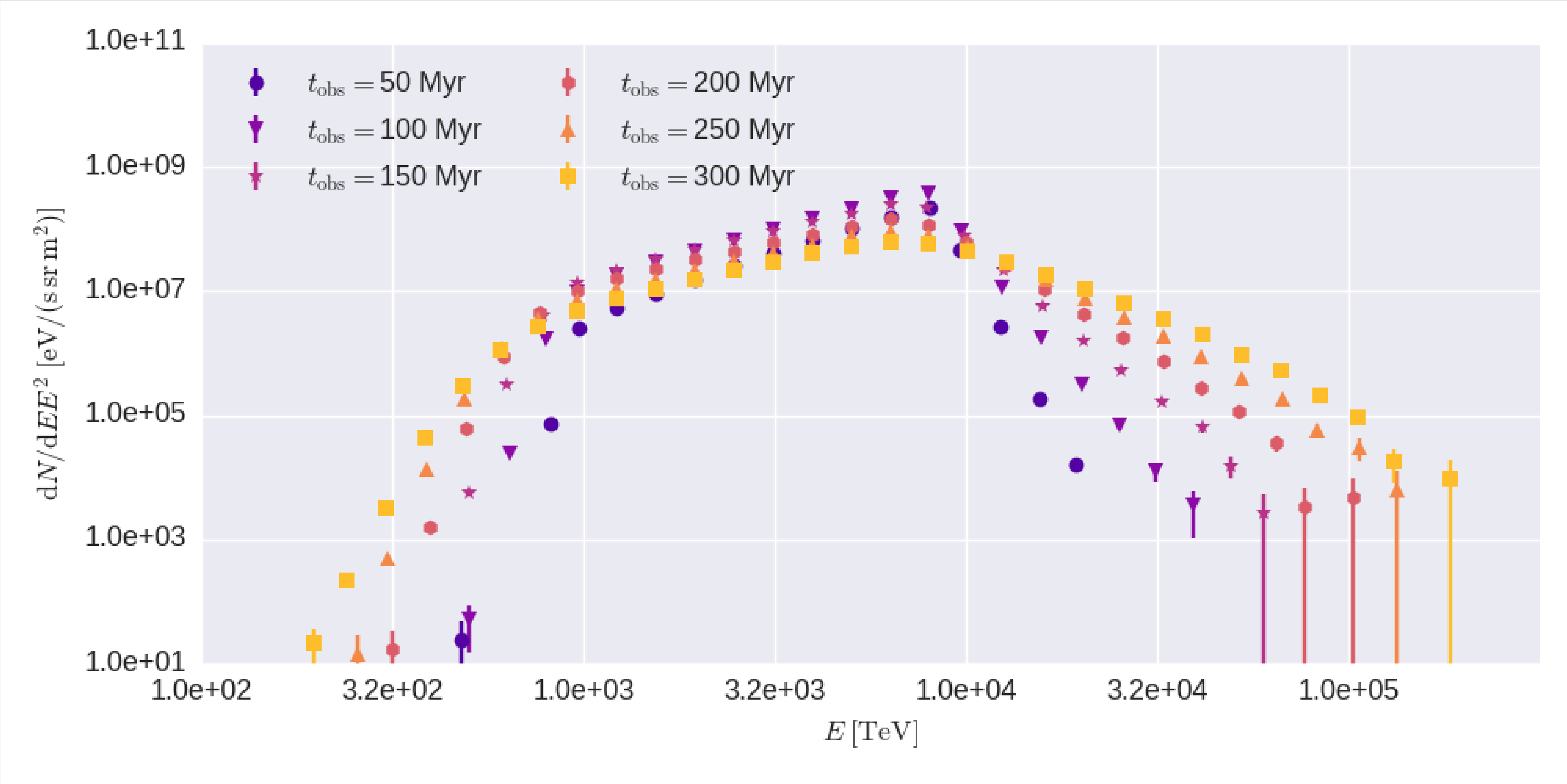

Fig 12: Spectrum including statistical errors.

4 Time Evolution $\Delta t = 100$ Myr; $\delta = 0.5$

Archmedean spiral – 3 dimensional ; $\epsilon = 0.1$

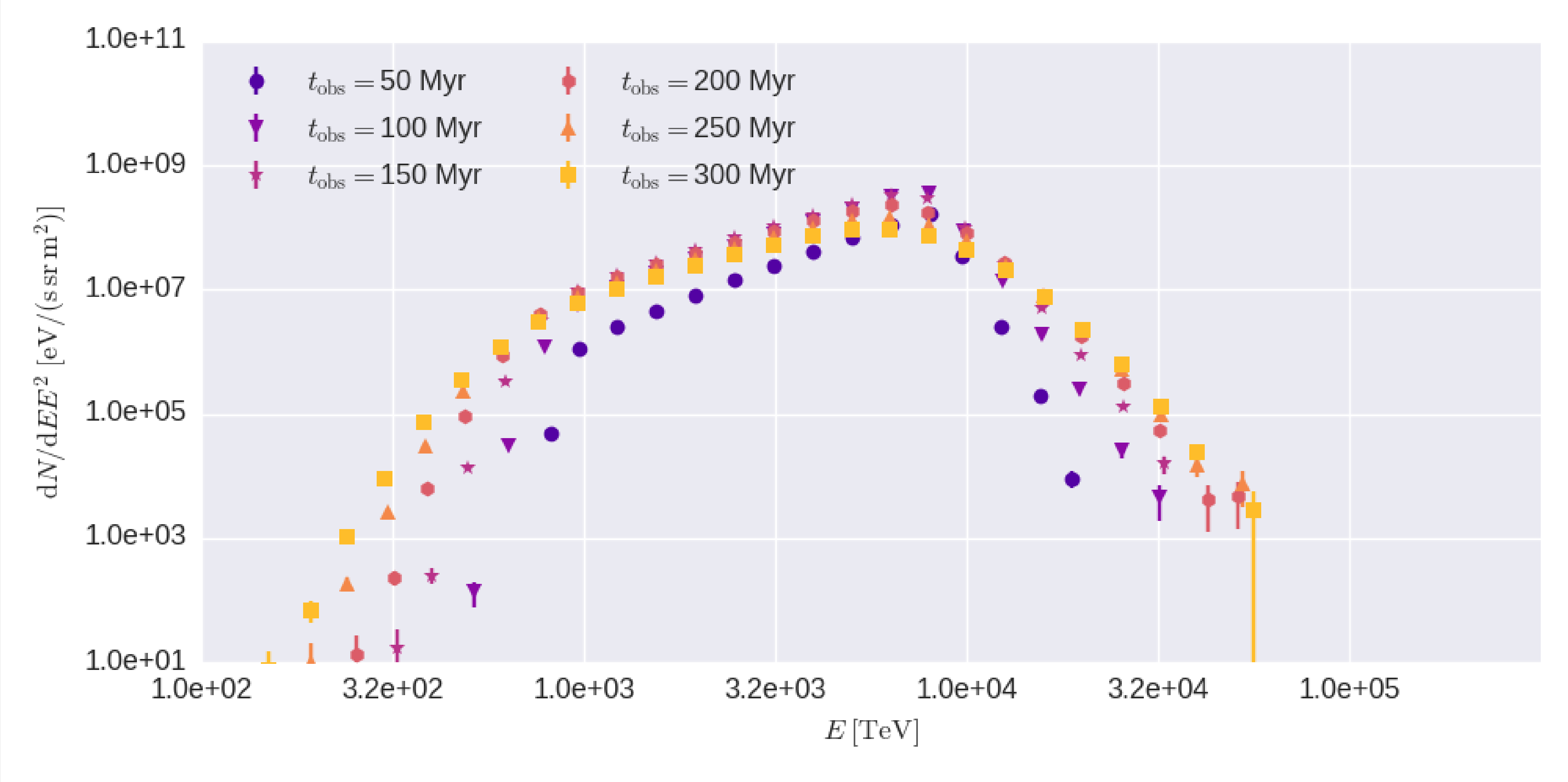

Fig 13: Spectrum including statistical errors.

Results – Arrival $\delta = 0.5, \epsilon = 0.$; Wind

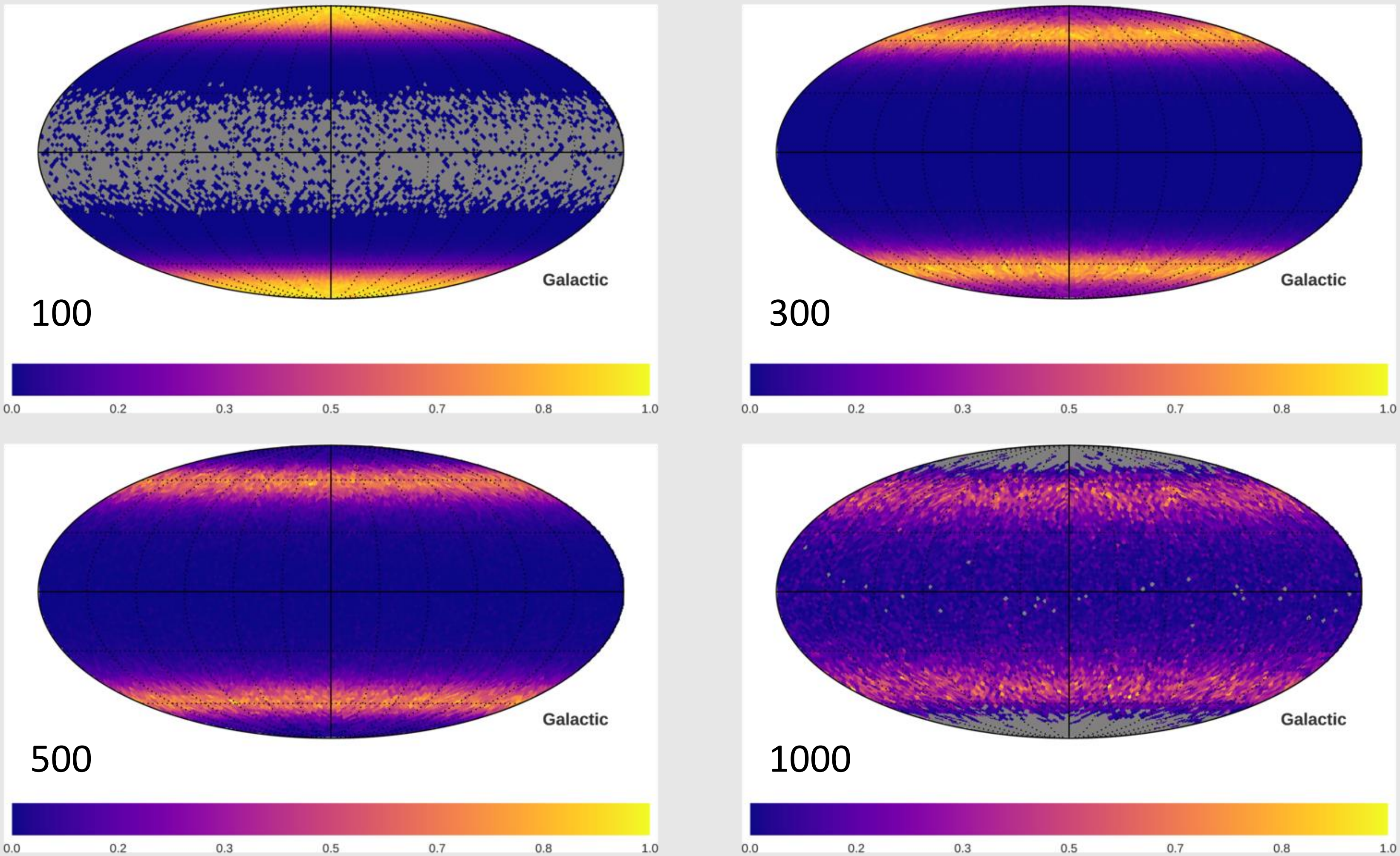

Fig 14: Arrival direction assuming pure parallel diffusion. Clear ring structure is visible

Results – Arrival $\delta = 0.5, \epsilon = 0.1$; Wind

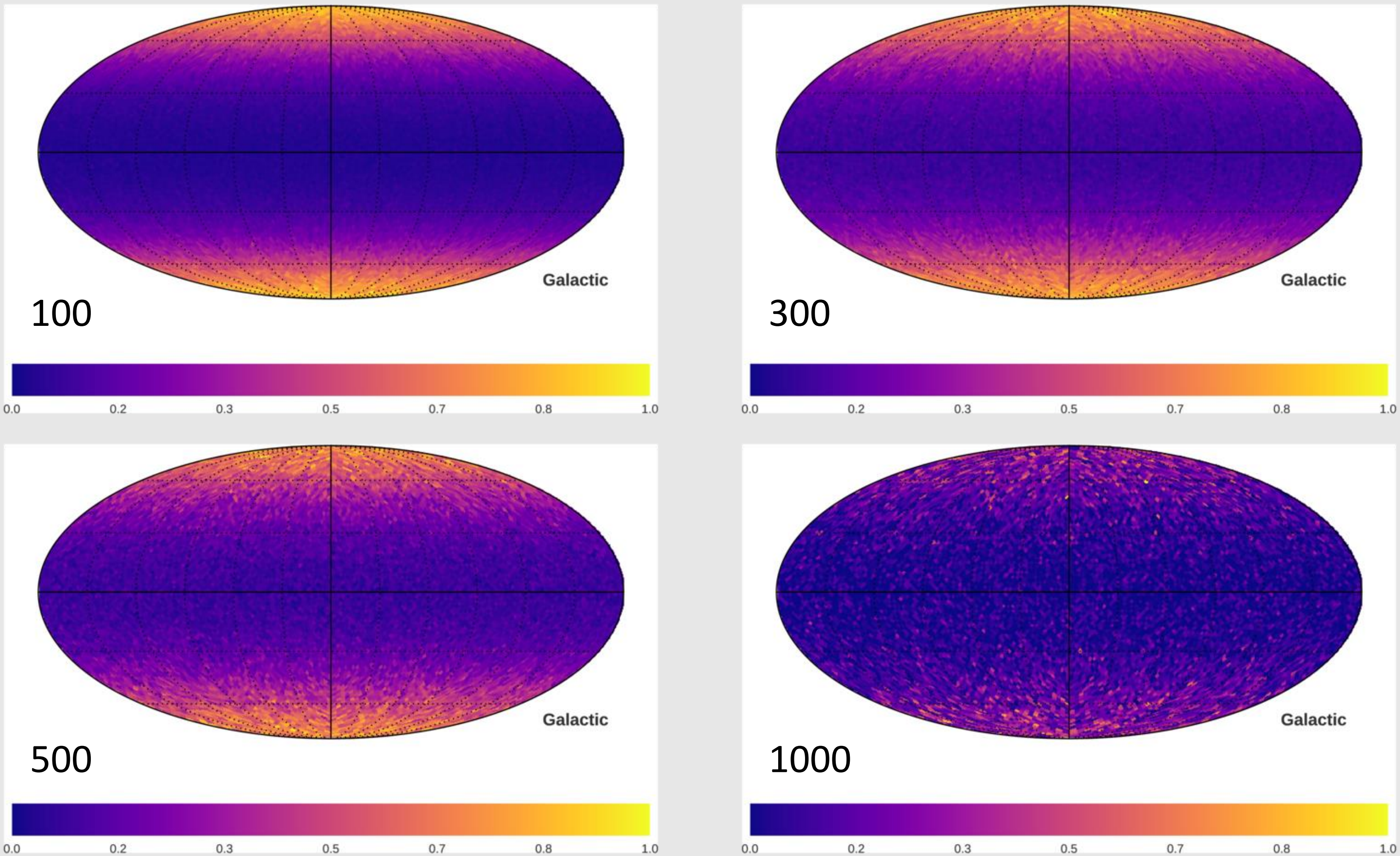

Fig 15: Allowing also for perpendicular diffusion leads to maximum at the poles.

5 Summary

- Observation challenge theoretical models
- Complex anisotropic (space dependent) diffusion tensors, advection and interaction models are needed
- CRPropa 3.1 uses anisotropic diffusion tensors in arbitrary background fields. Simple advection models are also included.
- CRPropa 3.1 uses SDE and is therefore trivial to parallelize on huge Clusters
- Not yet a finished ‚Out-of-the-box-solution' like GALPROP, …
  …but easy to extend to fit your needs.

5 Outlook

- Further investigation of the Galactic termination shock, e.g. propagation of CRs also through the Galaxy
- Quantitative investigation of anisotropy, composition and spectrum with realistic magnetic field/diffusion tensor
- Realistic neutrino and gamma maps for the Galaxy (once hadron-hadron interactions have been implemented)
- Investigation of Fermi bubbles and WMAP haze possible, with precise calculation of implied neutrino signatures

Backup

Galactic Termination Shock
Simulation details

Model Assumption

Symmetry

- Radial / Archmedean spiral

Diffusion

- D$\propto E^{\delta}$
- $D_0 = 10^{28} \frac{cm^2}{s}$

Advection

- $v_0 = 600 \frac{km}{s}$
- $r_0 = 250\ kpc$

Boundaries

- $r_{obs} = 10\ kpc$
- $r_{loss} = 350\ kpc$

Simulation details

- $N = 10^7 - 8.5 \cdot 10^8$
- $\tau_{CPU} = O(10)h - O(1000)h$

Observation

Observation – Energy Spectrum

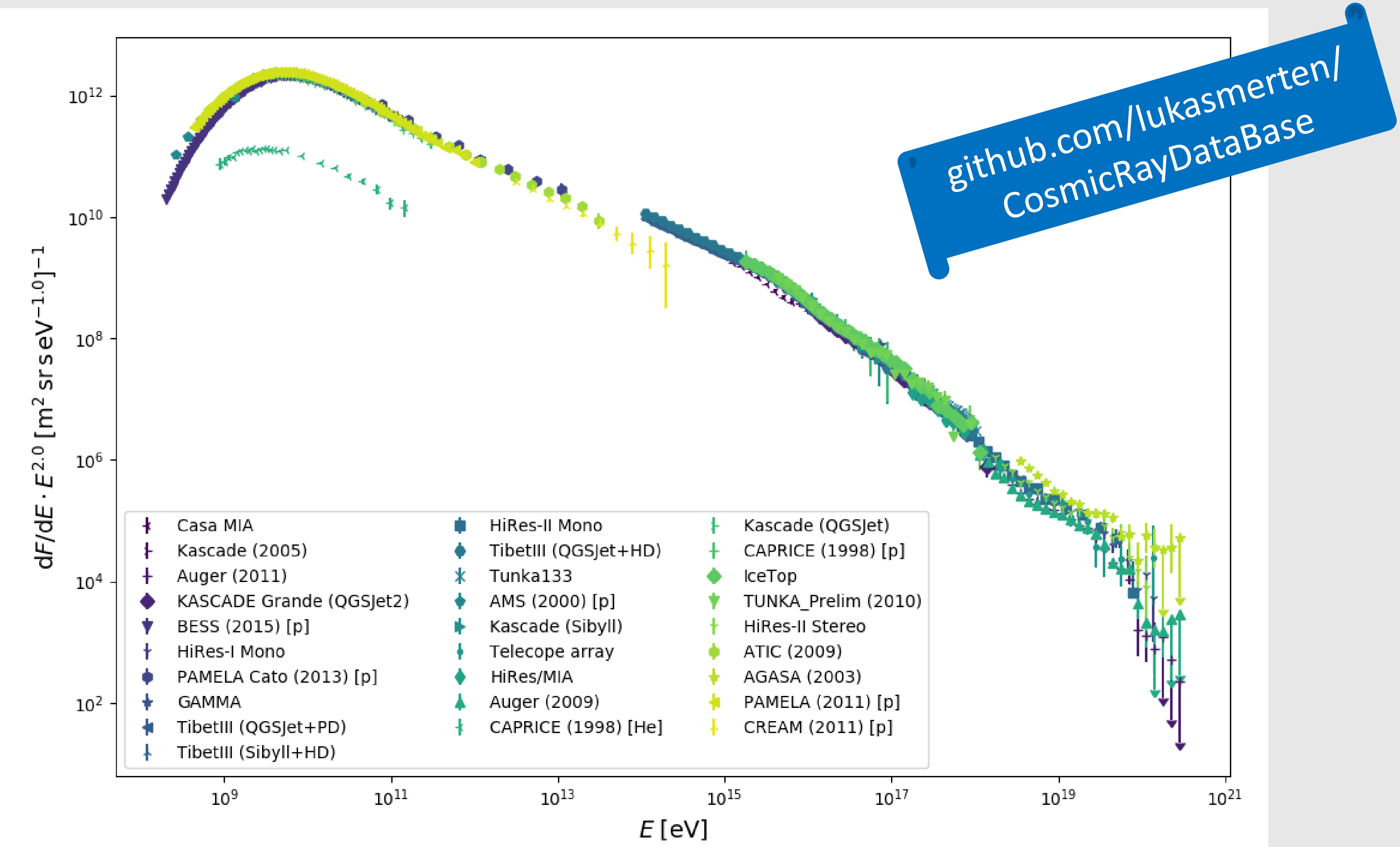

Fig 2. The energy spectrum of Cosmic rays.

Observation - Composition

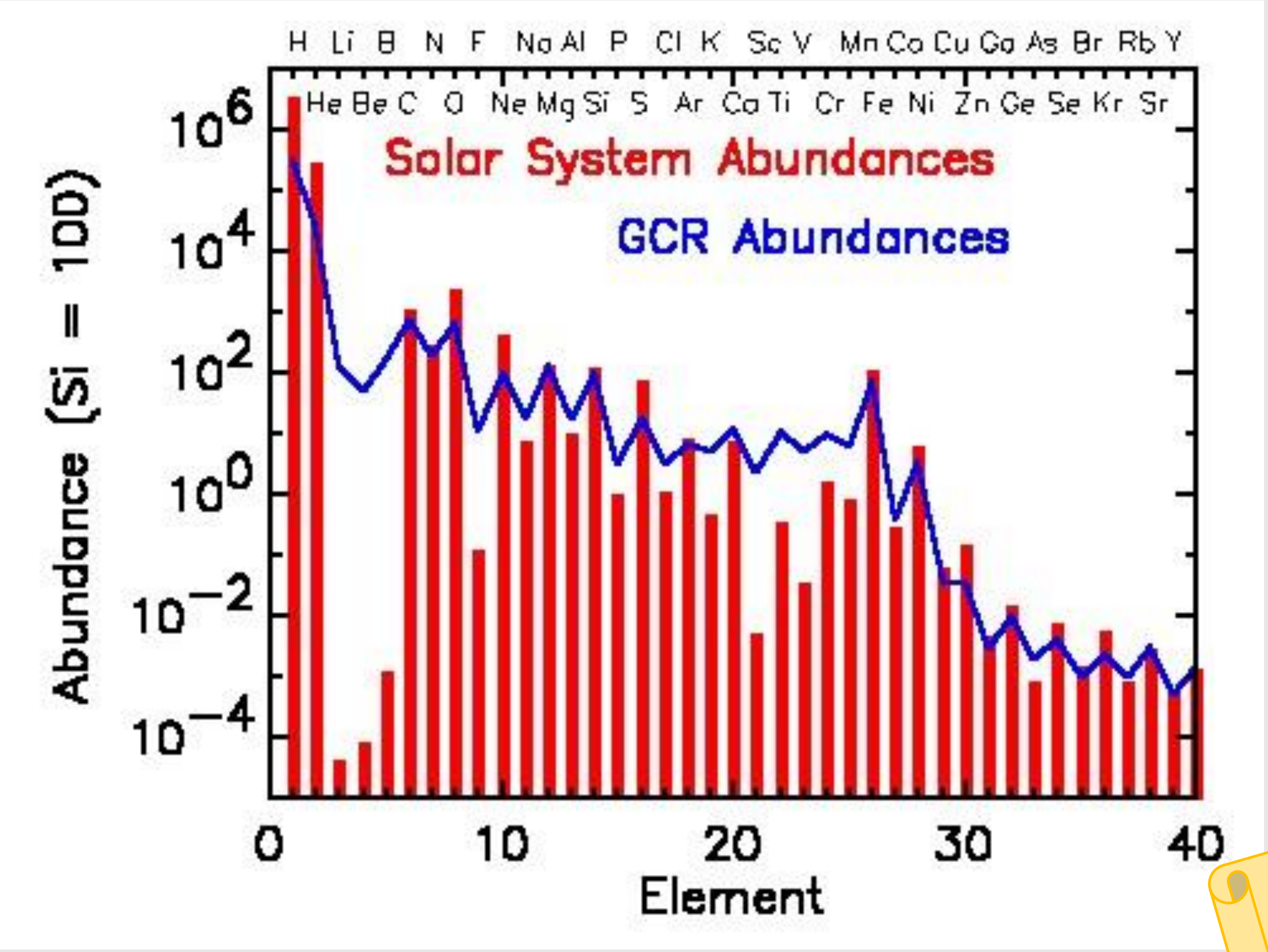

Fig 3. Boron to carbon ratio as a measure for the column depth.

NASA. Imagine the Universe. access: (23.02.2015)

Observation – B/C ratio

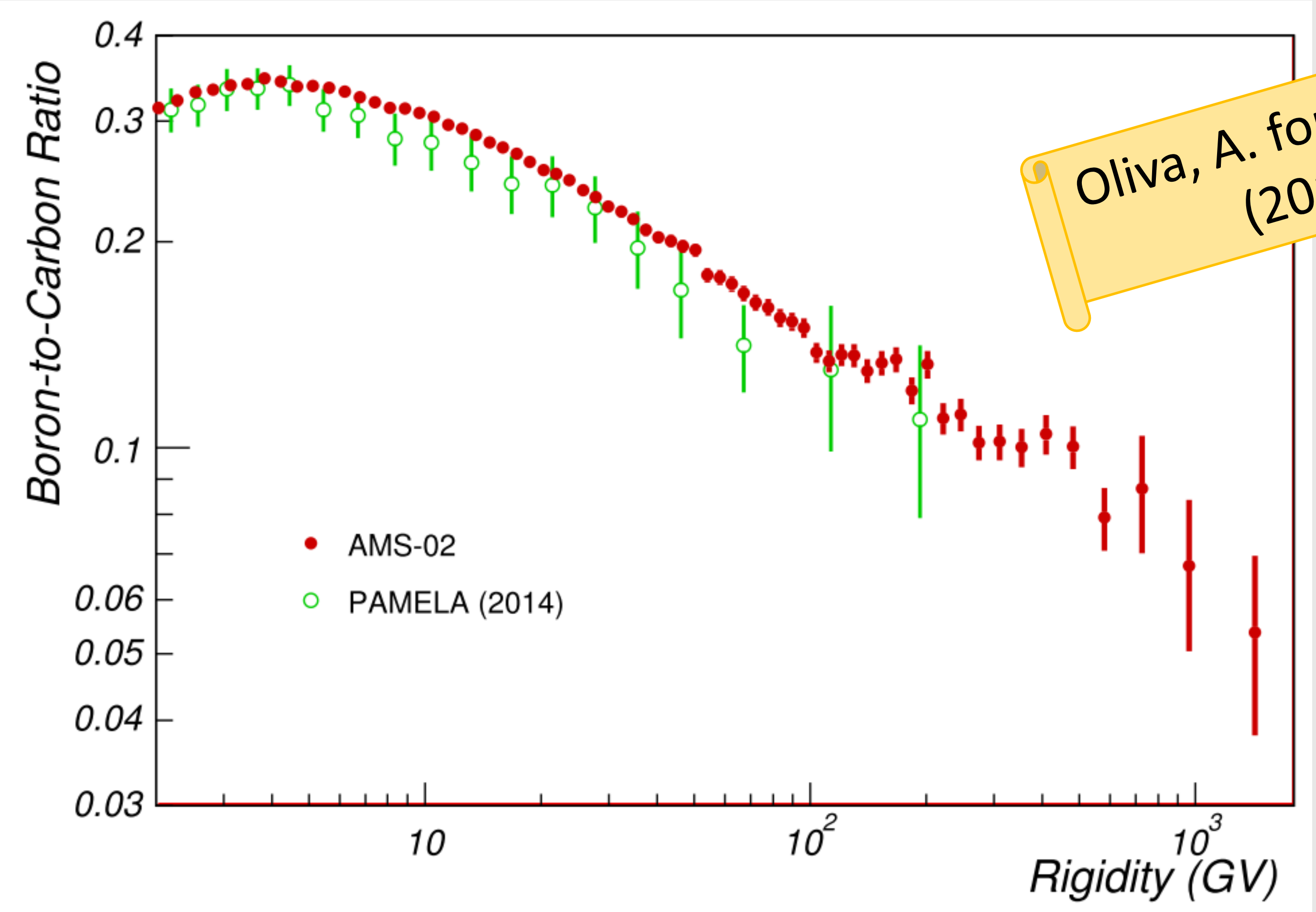

Oliva, A. for AMS-02 (2015)

Fig 3. Boron to carbon ratio as a measure for the column depth.

Observation – Arrival Directions

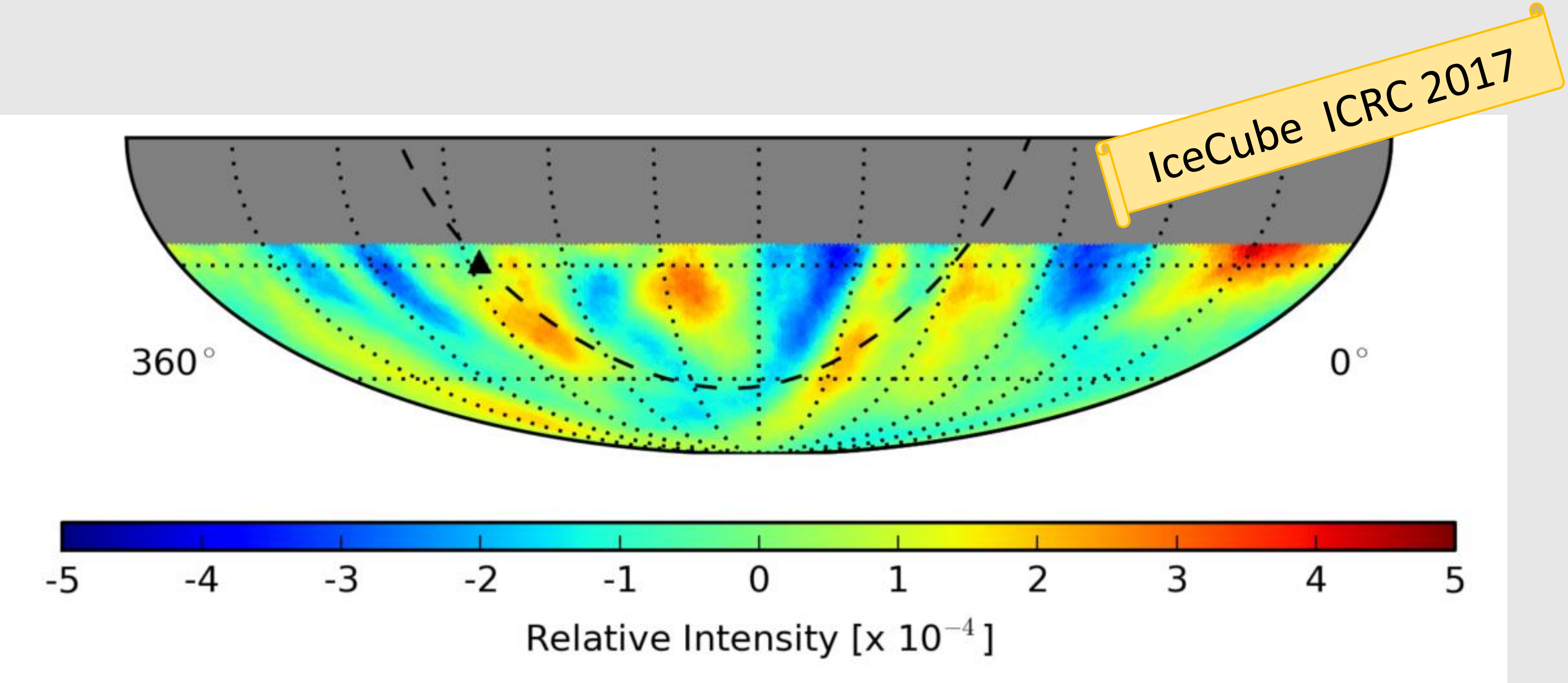

Fig 4. Cosmic ray arrival anisotropy at a median energy E=20 TeV after the subtraction of the best fit dipole and quadrupole.

SDE
Mathematics

Stochastic Differential Equation

Langevin Equation

$$\frac{\mathrm{d}x}{\mathrm{d}t} = a(x,t) + b(x,t)\xi(t)$$

Stochastic Integral Equation

$$x(t) = x(0) + \int_{t_0}^{t} a[x(s),s]\,\mathrm{d}s + \int_{t_0}^{t} b[x(s),s]\,\mathrm{d}W(s)$$

- These equations can be treated mathematically consistently.
- Numerical algorithm to solve them are available.

From Fokker-Planck Equ. to SDE

General Fokker-Planck Equation

$$\frac{\partial n(x,t;y,t')}{\partial t} = -\sum_i \frac{\partial}{\partial x_i}[A_i(x,t)n(x,t;y,t')] + \frac{1}{2}\sum_{i,j}\frac{\partial^2}{\partial x_i \partial x_j}[B_{ij}(x,t)n(x,t;y,t')]$$

Corresponding Stochastic Differential Equation

$$\mathrm{d}r_\nu = A_\nu \,\mathrm{d}t + D_{\nu\mu}\,\mathrm{d}\omega^\mu$$

Calculation of stochastic tensor D

$$(\kappa + \kappa^t) = DD^\dagger$$

In the case of decoupled momentum und spatial operators
And diagonal diffusion tensor

$$D_{ij} = \delta_{ij}\sqrt{2\kappa_{ij}}, \qquad D_{qq} = \sqrt{2\kappa_{qq}}$$

Integration scheme

$$\vec{x}_{n+1} = \vec{x}_n + D_r\,\Delta\vec{\omega}_r$$
$$= \vec{x}_n + \left(\sqrt{2\kappa_{||}}\,\eta_{||}\,\vec{e}_t + \sqrt{2\kappa_{\perp,1}}\,\eta_{\perp,1}\,\vec{e}_n + \sqrt{2\kappa_{\perp,2}}\,\eta_{\perp,2}\,\vec{e}_b\right)\sqrt{h}$$

- Magnetic field line implementation (e.g. JF12 field) is not trivial.
- Calculation of the local trihedron is the crucial part.

- Use adaptive field line integration → e.g. Cash-Karp algorithm.

$$\vec{r}_{end} = \vec{r}_{start} + \int_0^L \vec{B}/B\,\mathrm{d}s$$

$$\vec{r}_{end} = \vec{r}_0 + \sum_{j=0}^{2^n-1} \int_{2^{-n}L\,j}^{2^{-n}L\,(j+1)} \vec{v}(s)\,\mathrm{d}s$$

SDE and FPE

Ito's lemma leads to equivalence between stochastic differential equation (SDE) and Fokker-Planck transport equation (FPE)

$$\frac{\partial \Psi(r,t)}{\partial t} = \nabla \cdot \left(D \cdot \nabla \Psi(r,t)\right) + S(r,t)$$

$$dr = A\,dt + B\,d\omega \qquad with: d\omega = \eta\sqrt{dt}$$

$$B = \sqrt{2 \cdot D},\ A = 0$$

Diffusion tensor is diagonal in frame with $\vec{B} = B_0 \cdot \vec{e_z}$

$$D = \begin{bmatrix} \kappa_{perp,1} & 0 & 0 \\ 0 & \kappa_{perp,2} & 0 \\ 0 & 0 & \kappa_{par} \end{bmatrix} \qquad with: \kappa_{perp,1} = \kappa_{perp,2}:$$

CRPropa

CRPropa: Interactions

Nucleons

- ElectronPairProduction (Bethe Heitler)
- PhotoPionProduction
- PhotoDisintegration
- Nuclear Decay

Electro-Magnetic

- EMPairProduction
- EMDoublePair-Production
- EMTripletPairProduction
- InverseCompton-Scattering

General

- Redshift (accounts for adiabatic energy loss)
- SynchrotronRadiation

Performance

Performance

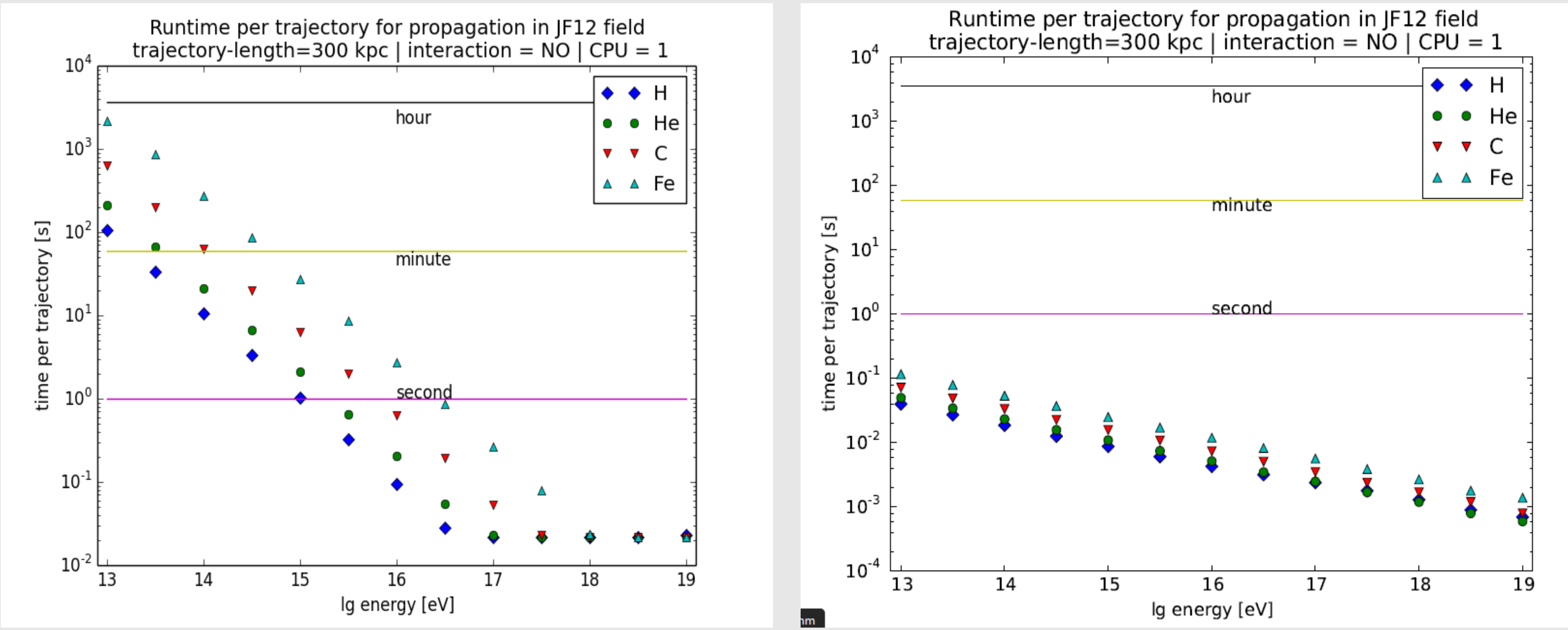

Fig 15: Comparison of computation times. Conventional CRPropa3 (left) and propagation with the DiffusionModule (right)

Problems with the JF12-field

Problem: Fixed step length

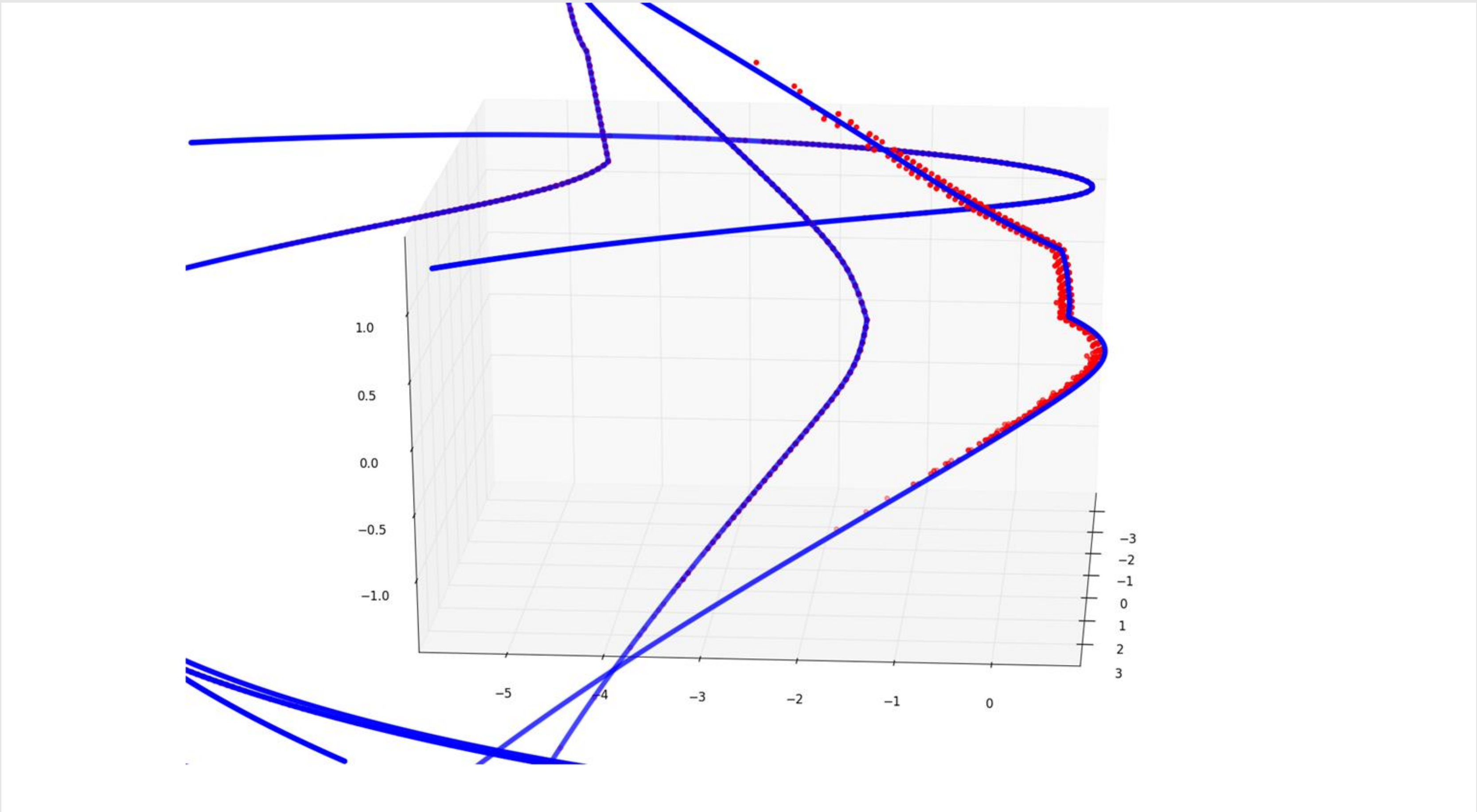

Fig 19: Magnetic field line (blue) and end position after diffusion process (red dots).

Deviation vectors

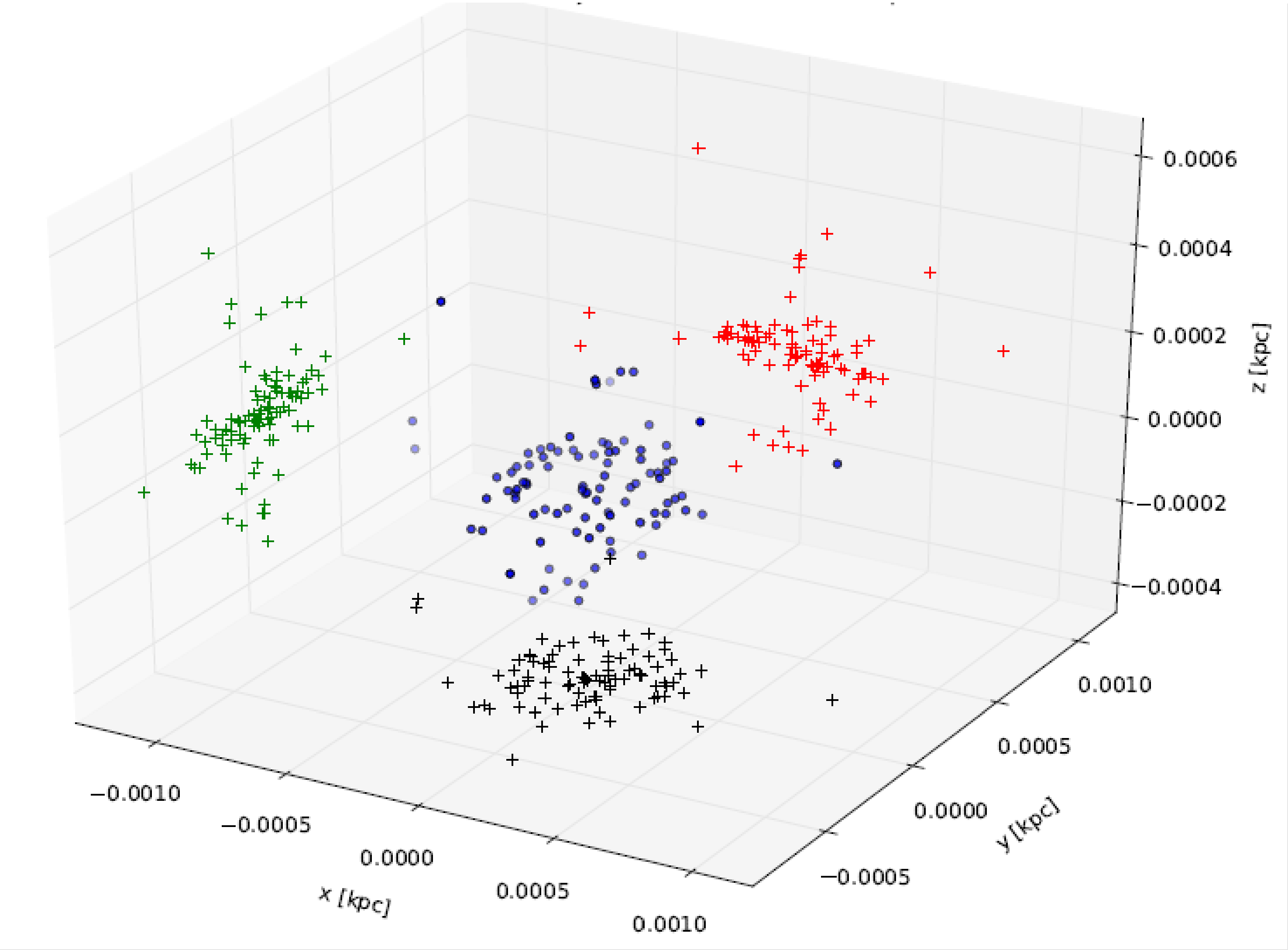

Fig 20: Ninty smallest deviation vectors for E=10TeV

Deviation from field line II

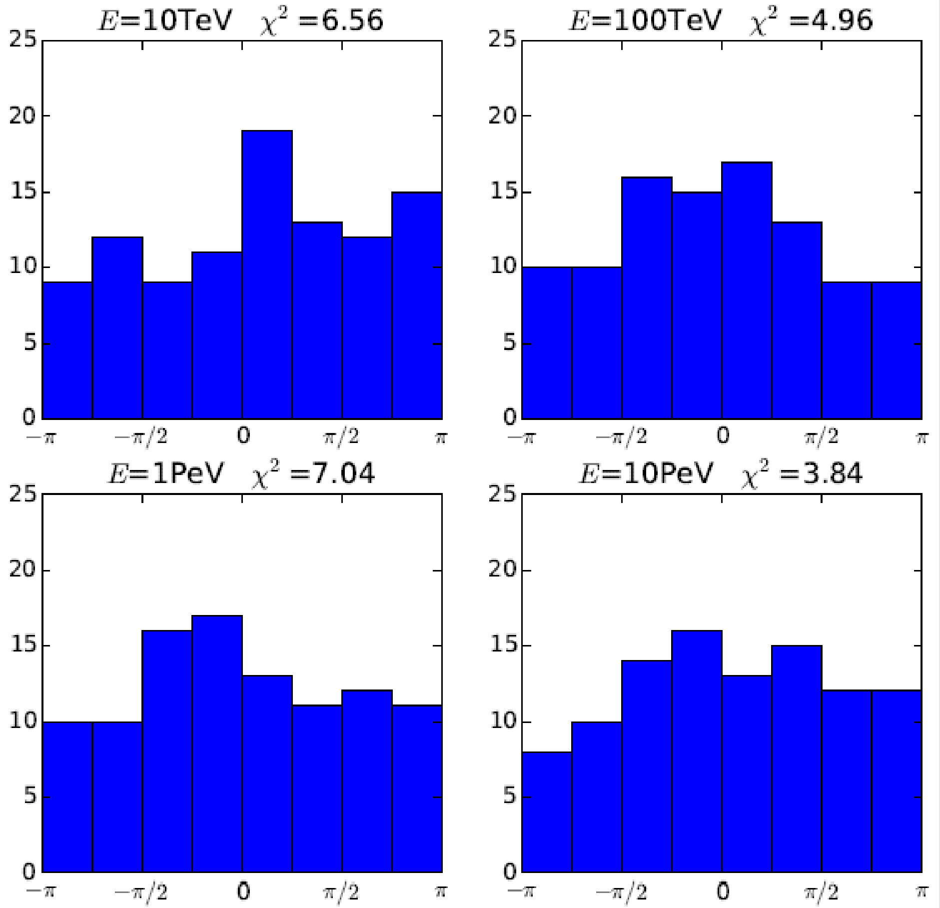

Fig 21: Deviation from ideal trajectory is uniformly distributed in Φ.

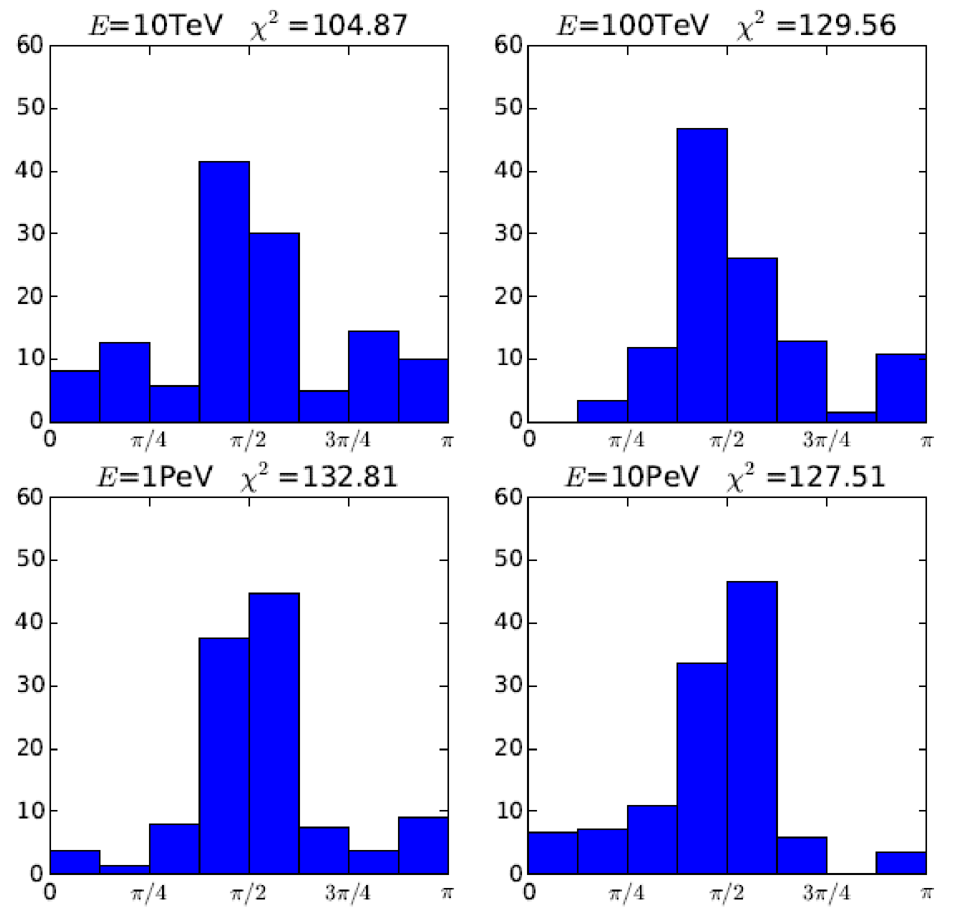

Fig 22: Deviation from ideal trajectory peaks around the plane perpendicular to magnetic field line.

Validation

Validation I

First test of the diffusion in a homogeneous magnetic background field.
A simple anisotropic diffusion tensor is implemented.

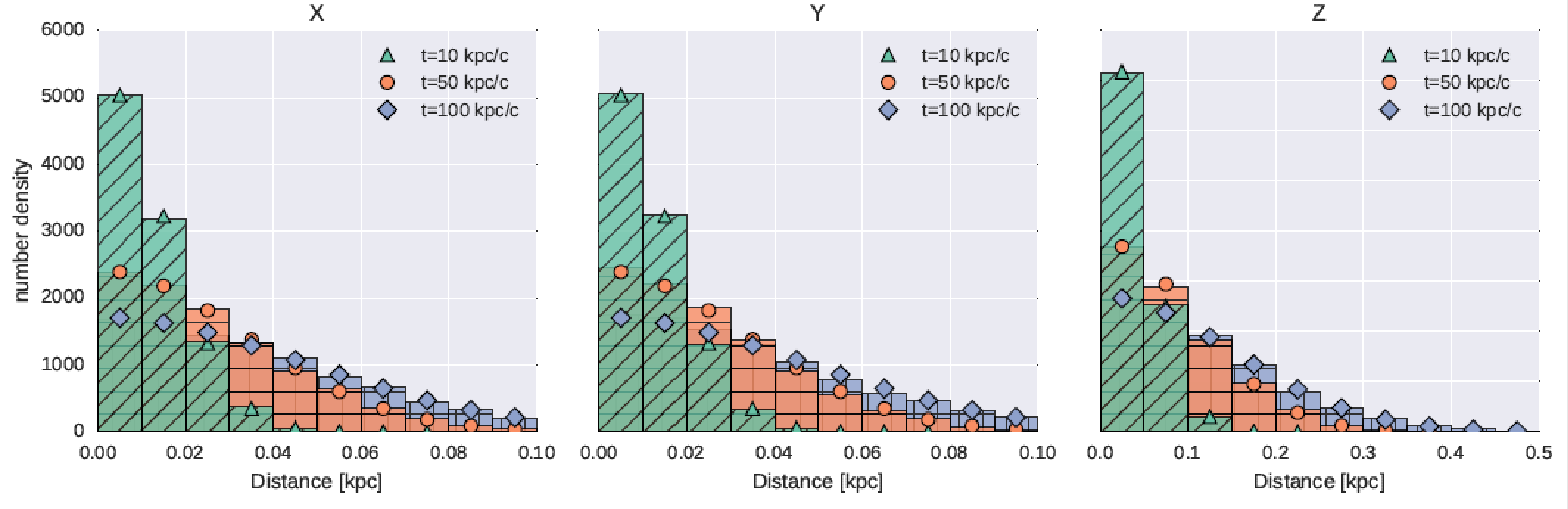

Fig 7. The algorithm reproduces the expected analytic results (simulation-barplot, theory-solid lines).

Stationary Test I

Stationary equation of anisotropic diffusion

$$-\nabla \cdot (\hat{\kappa} \nabla n(\vec{r})) = s(\vec{r})$$

Not possible?

Source term

$$s(\vec{r}) = \frac{4}{\pi^2} \left(\frac{2\kappa_{xx}}{4R^2} + \frac{\kappa_{zz}}{2H^2} \right) \cdot \cos\left(\frac{x\pi}{2R}\right) \cos\left(\frac{y\pi}{2R}\right) \cos\left(\frac{z\pi}{2H}\right)$$

Indirect solution

$$\frac{\partial n}{\partial t} = \nabla \cdot (\hat{\kappa} \nabla n) + s(\vec{r}) \delta(t - t_i)$$

$$n_{sim}(\vec{r}) = \sum_i n(t_i) h_i w$$

Stationary Test II

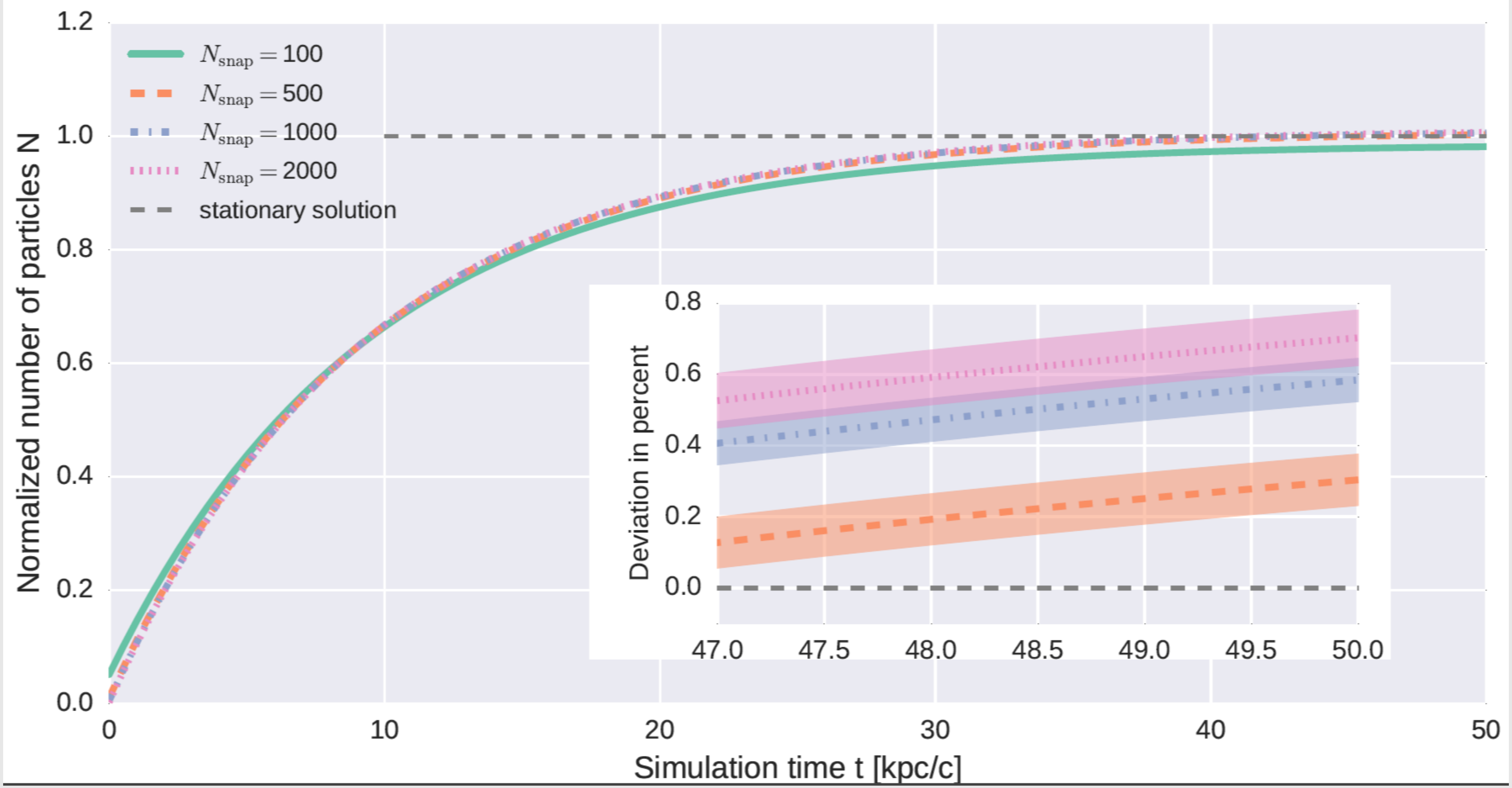

Fig 8. Total number density depending on maximum integration time for different numbers of snapshots.

Stationary Test III

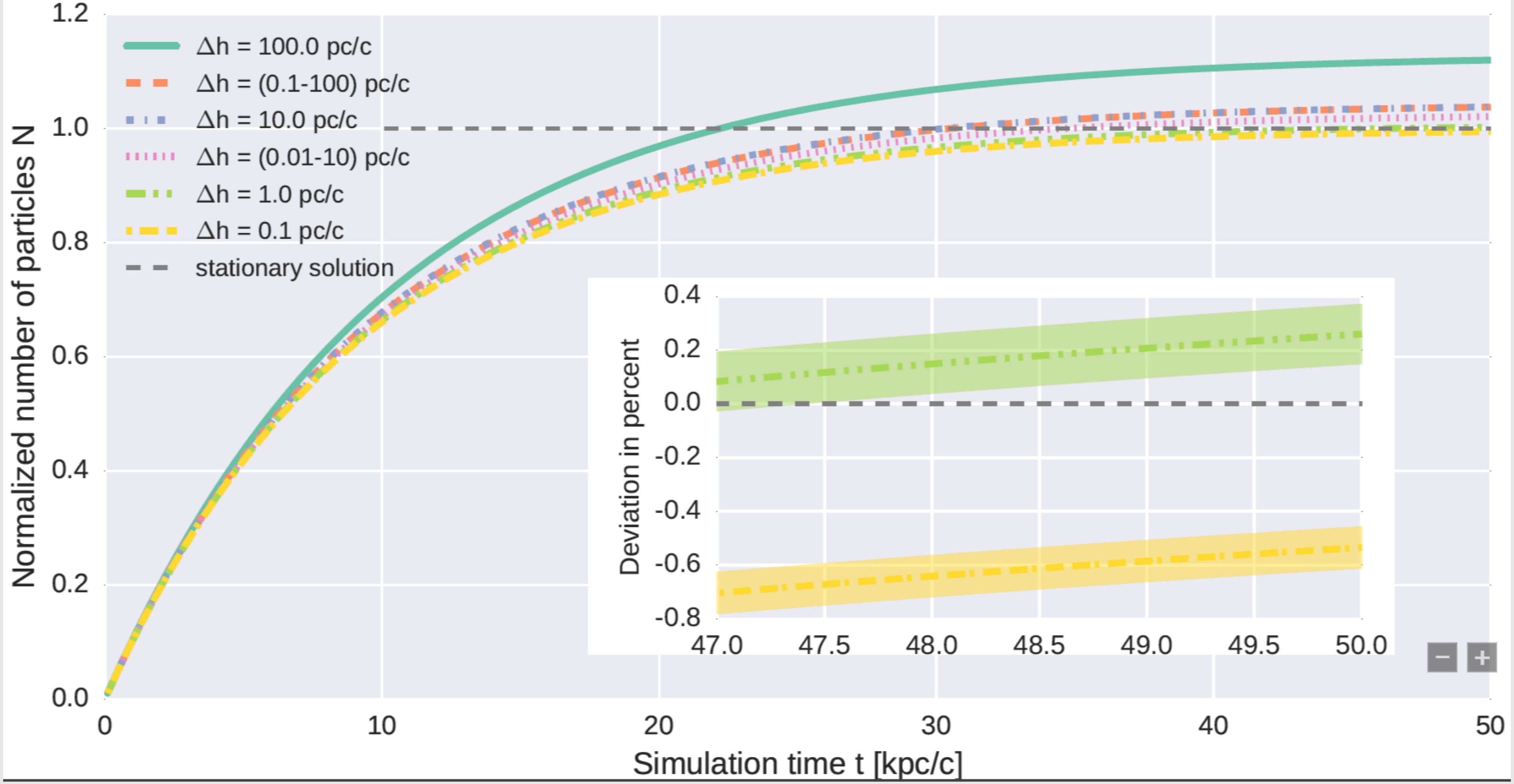

Fig 25. Total number density depending on maximum integration time for different integration time steps.

Validation IIa

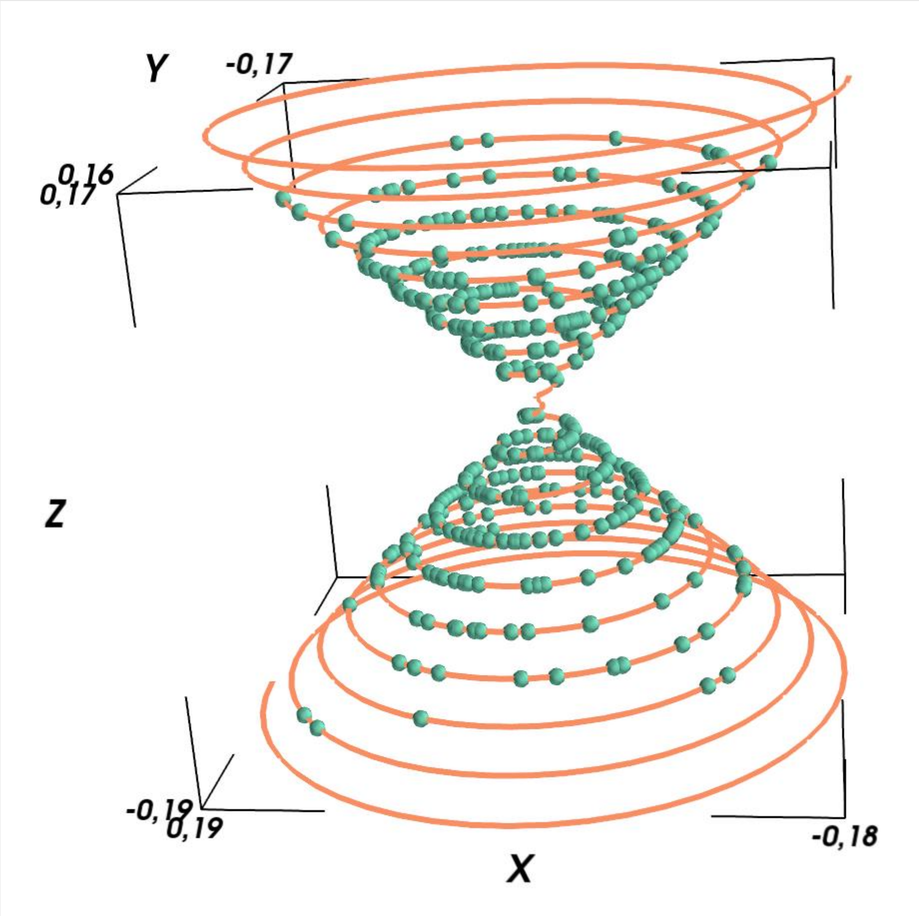

Fig 9: Example of a spiral field line and a sample of end positions.

- We test the accuracy of the algorithm in an artificial situation.
- A spiral with varying radius is used as the magnetic field line.
- The distance to the field line after the diffusion is taken as a measure for the algorithm accuracy.

Validation IIb

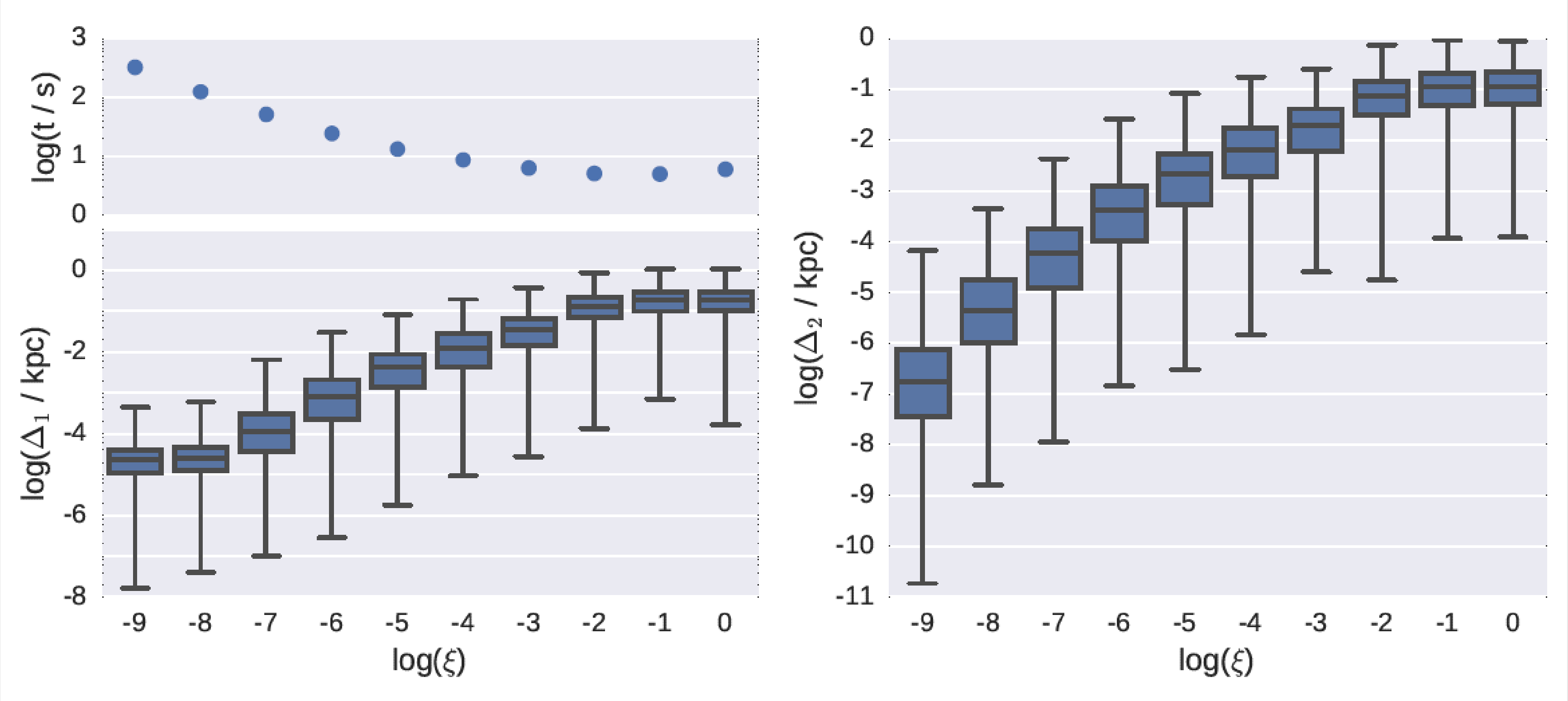

Fig 10: Results for the accuracy test. The algorithm allows a user chosen precision for a pure parallel diffusion.

Adiabatic Cooling

$$\frac{\partial n}{\partial t} + \vec{u} \cdot \nabla n = \nabla \cdot (\hat{\kappa} \nabla n) + \frac{1}{3} (\nabla \cdot \vec{u}) \frac{\partial n}{\partial \ln p} + S(\vec{x}, p, t)$$

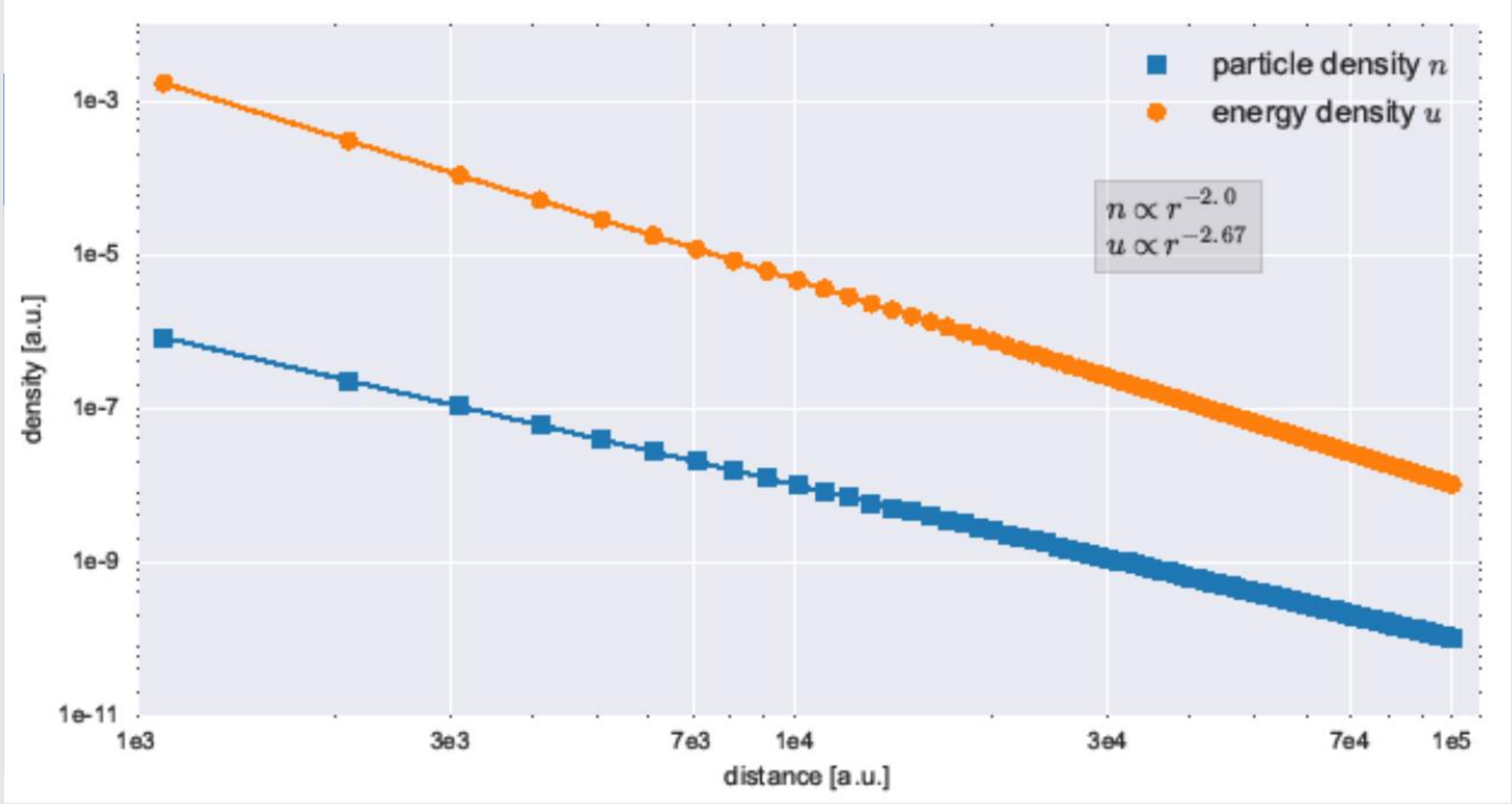

Fig 4. Particle and energy density for advective test case.

Examples

First applications – Rigidity

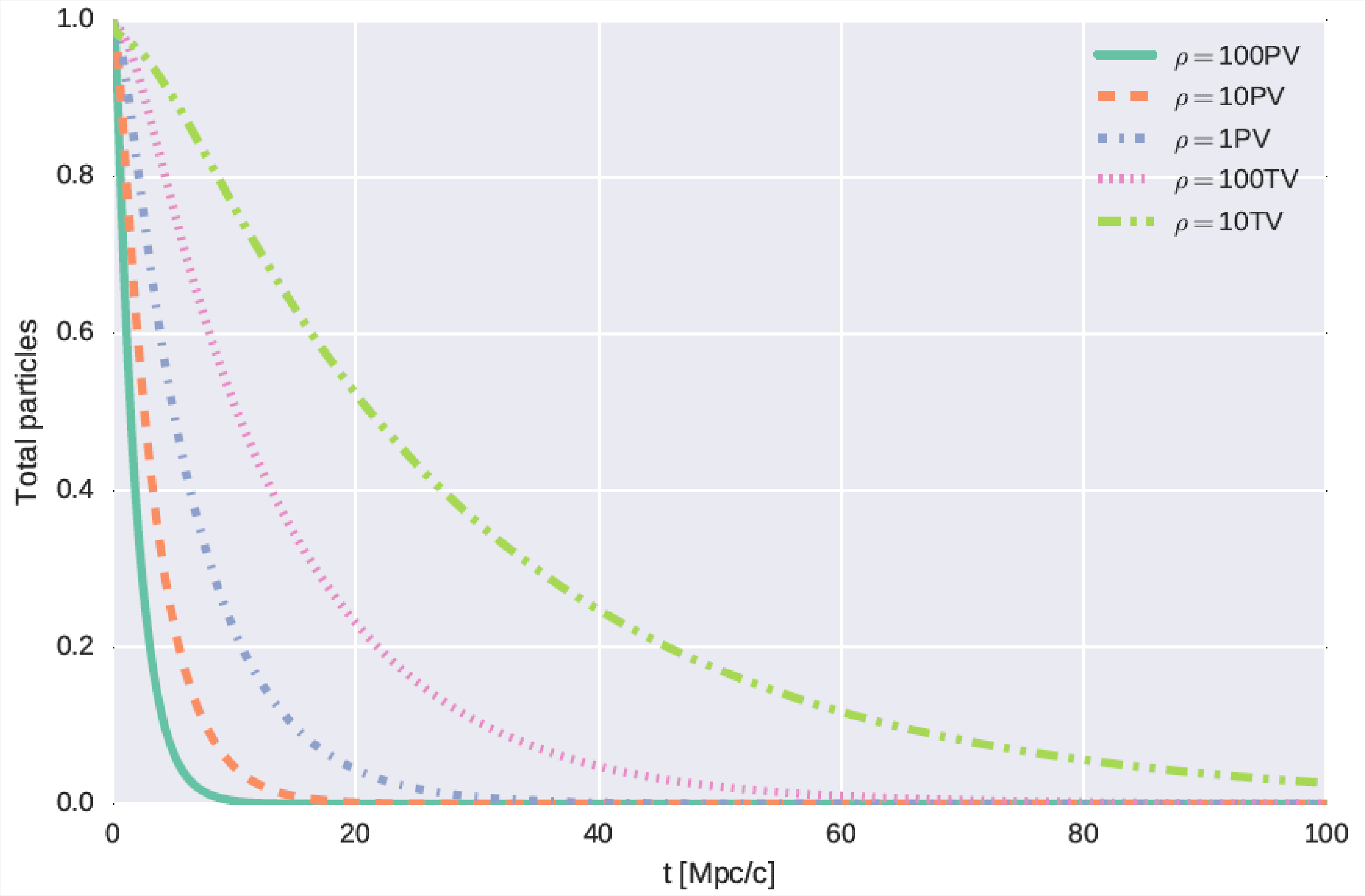

Fig 14: Time Evolution of the total particle number.

Continuous source

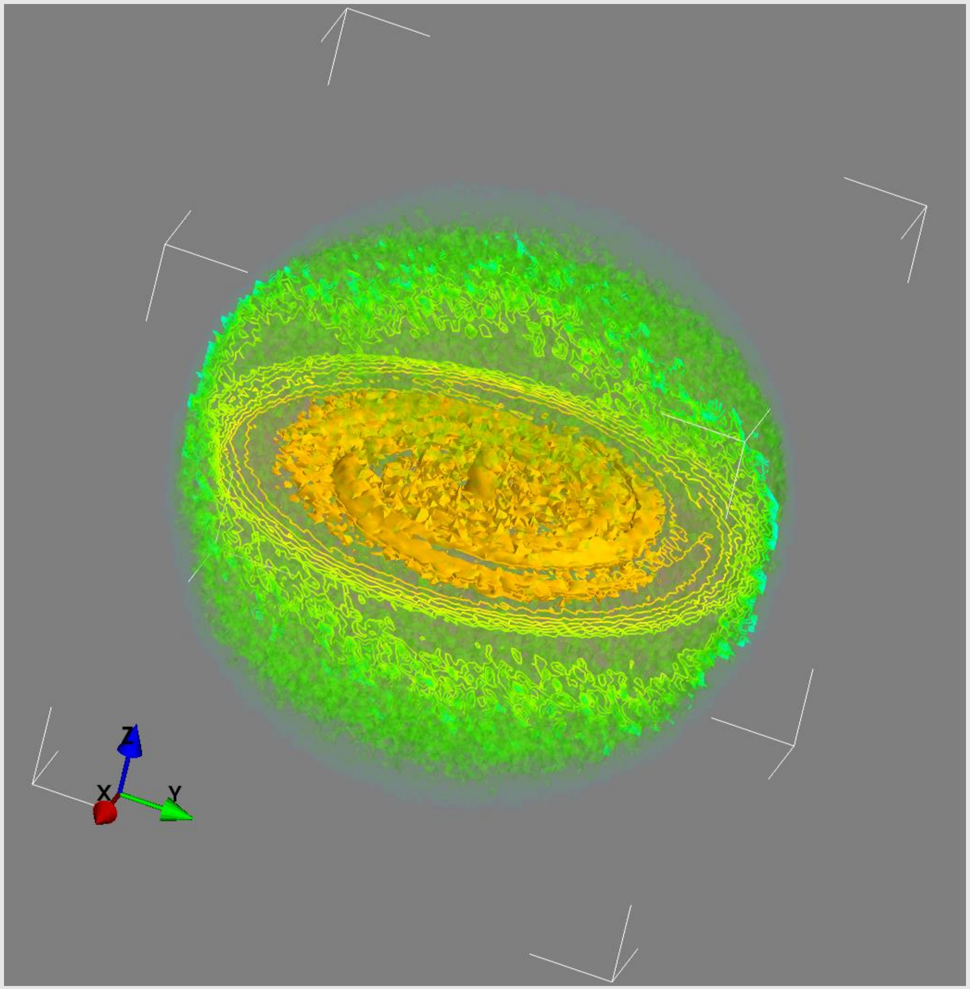

Fig 24: Cosmic ray density for continuous uniform emission inside the Galactic disc.

4 Time Evolution $\Delta t = 100$ Myr; $\delta = 0.5$

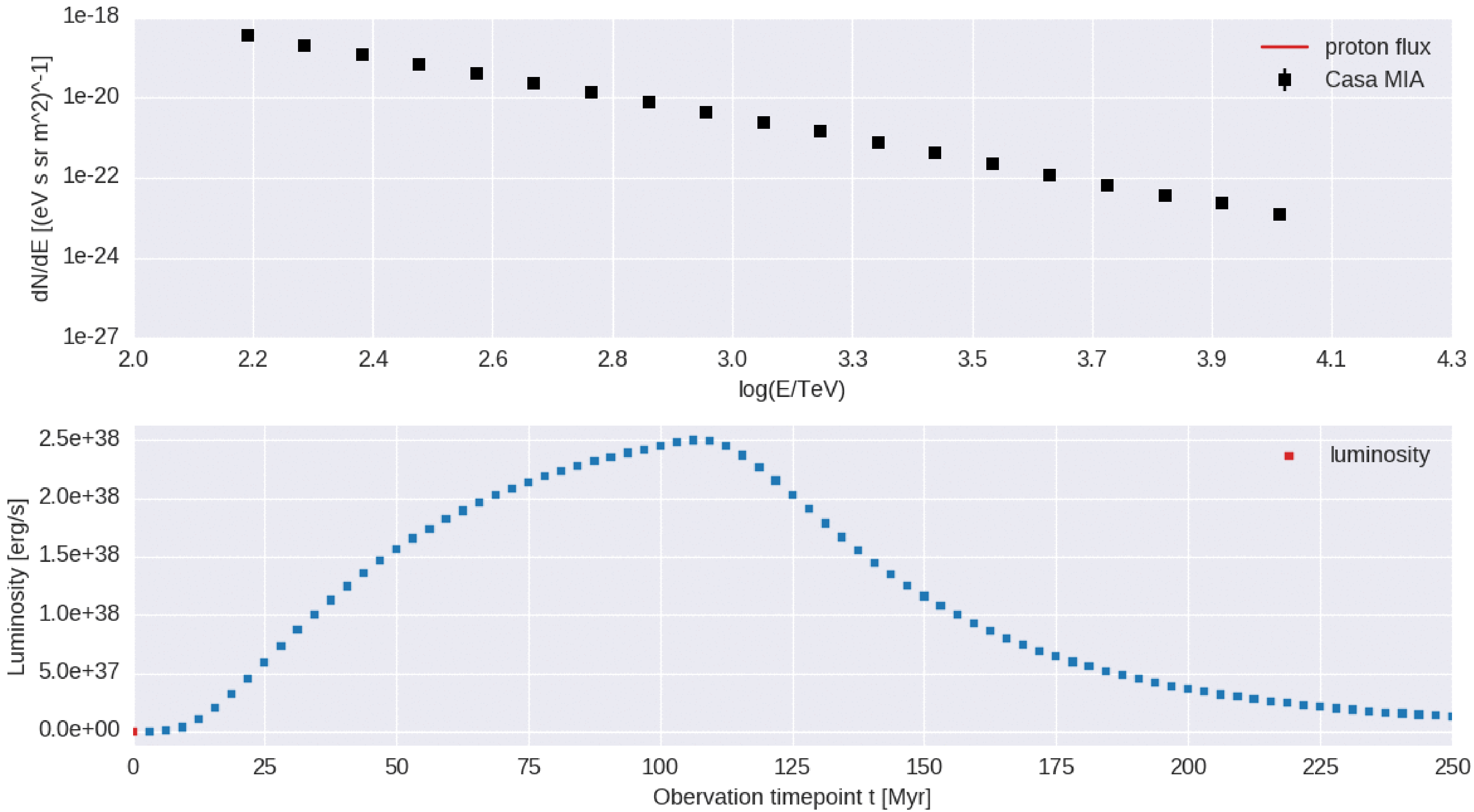

Time Evolution $\Delta t = 100$ Myr; $\delta = 0.3$

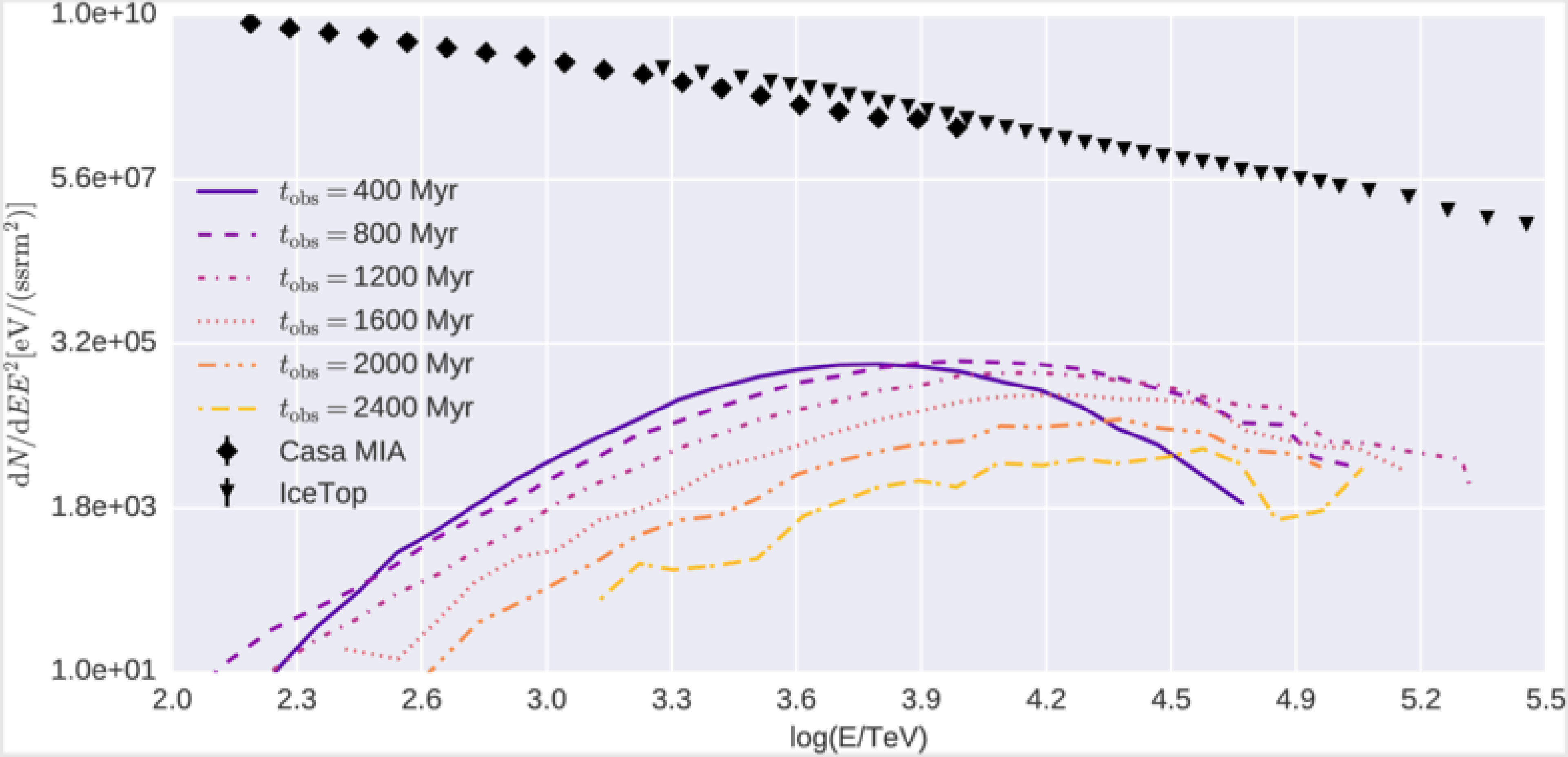

4 Time Evolution $\Delta t = 100$ Myr; $\delta = 0.4$

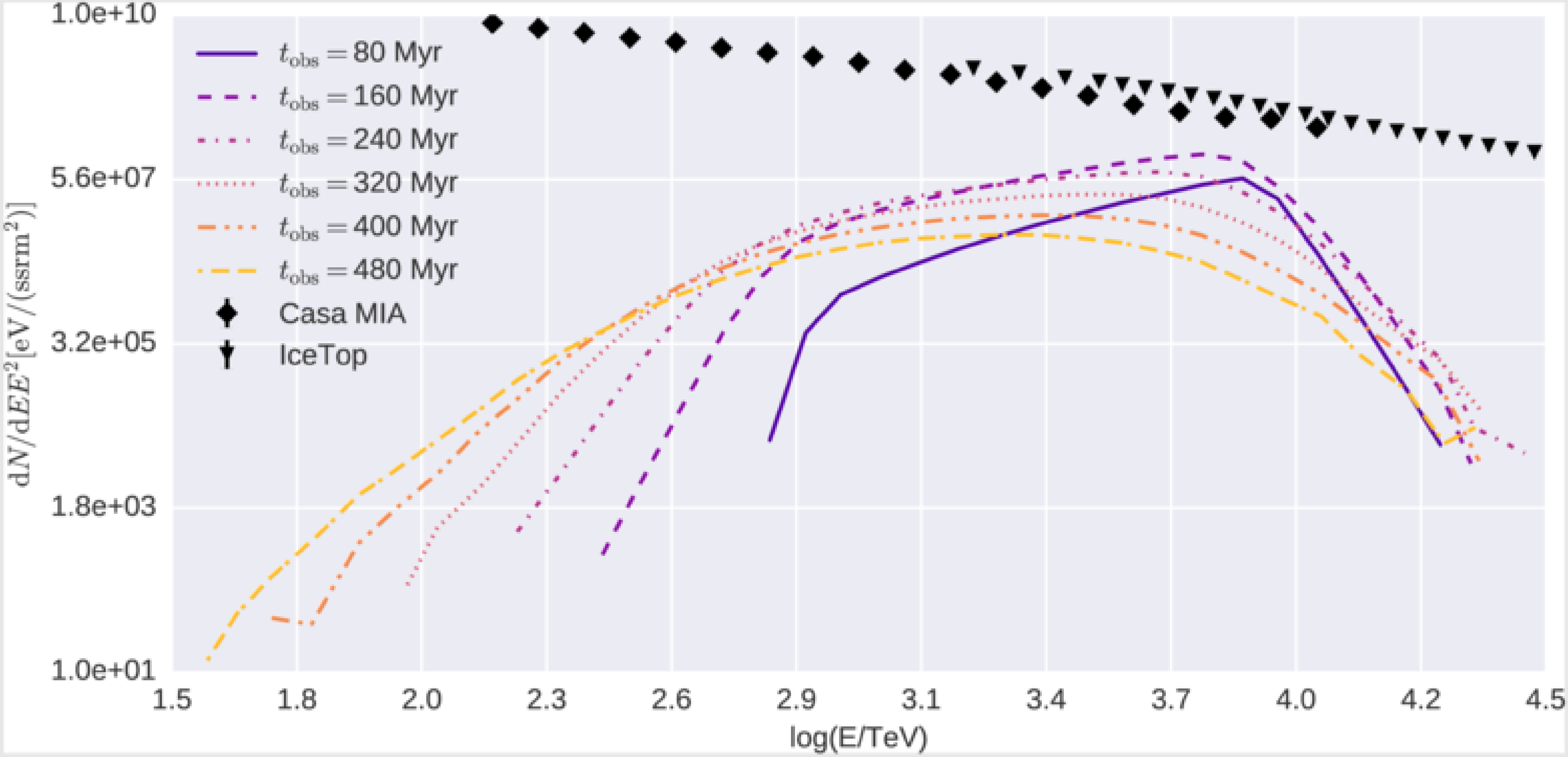

4 Time Evolution $\Delta t = 100$ Myr; $\delta = 0.5$

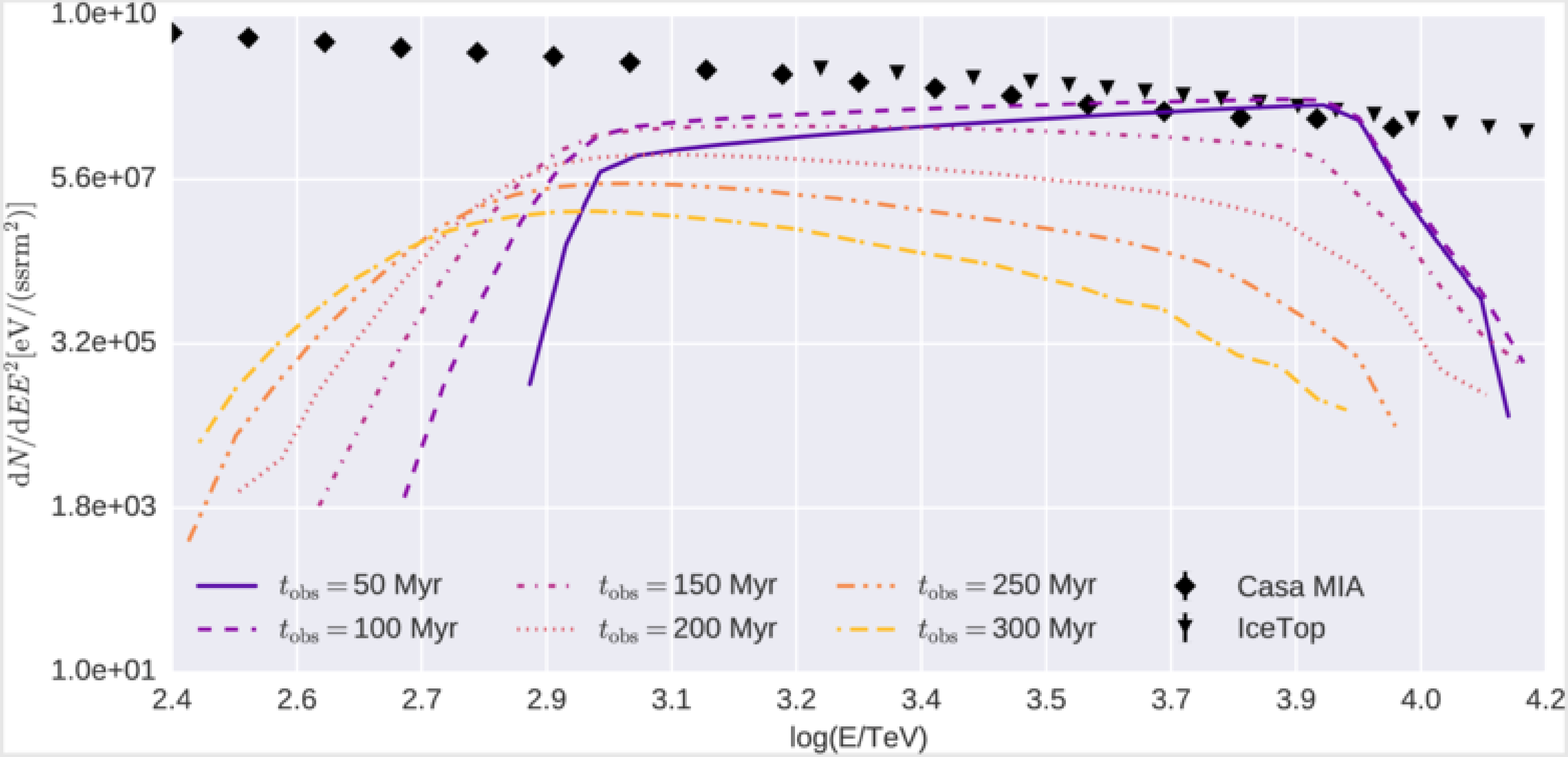

Time Evolution $\Delta t = 100$ Myr; $\delta = 0.6$

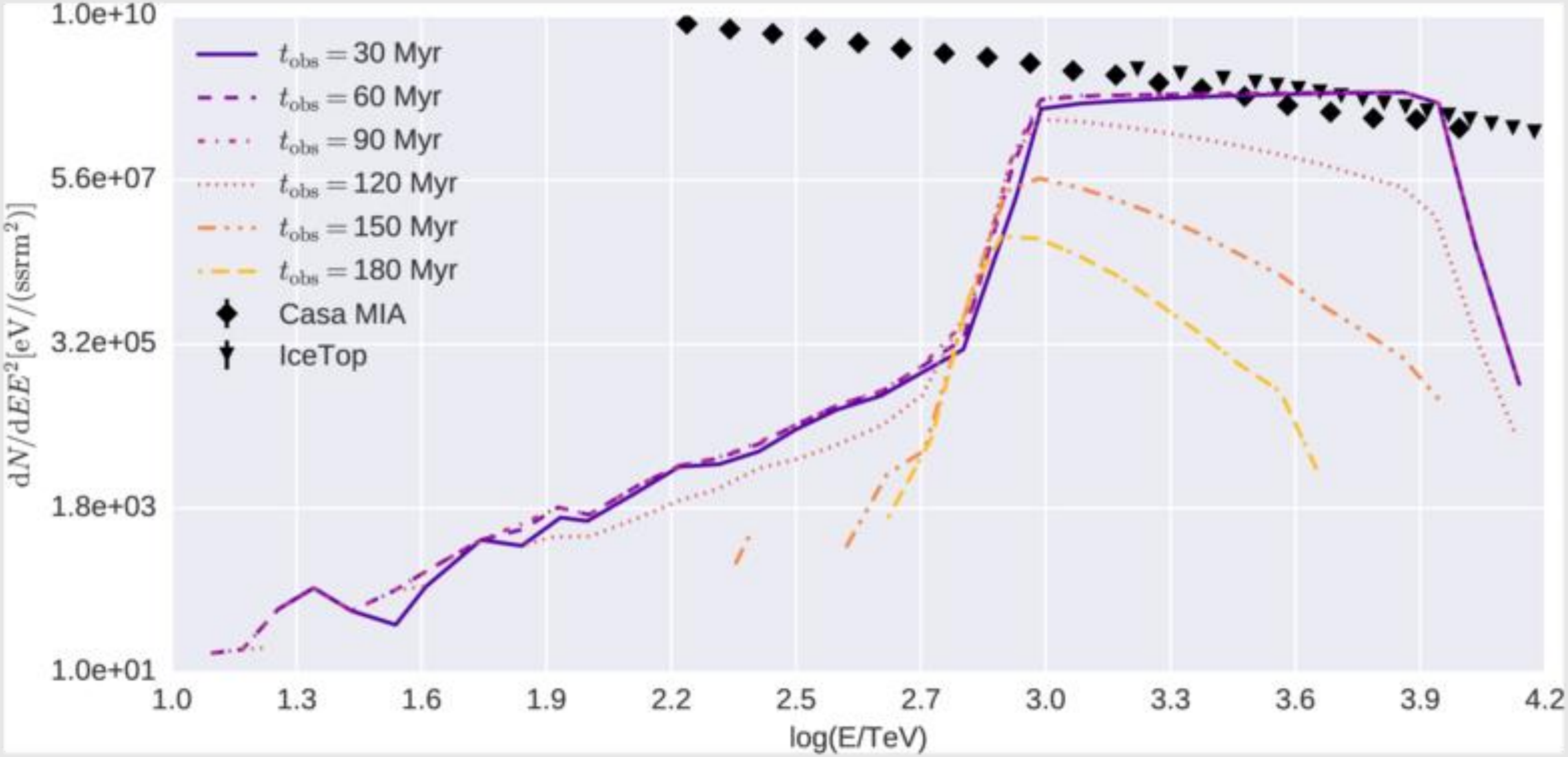

4 Arrival $\delta = 0.6, \epsilon = 0.$; Wind

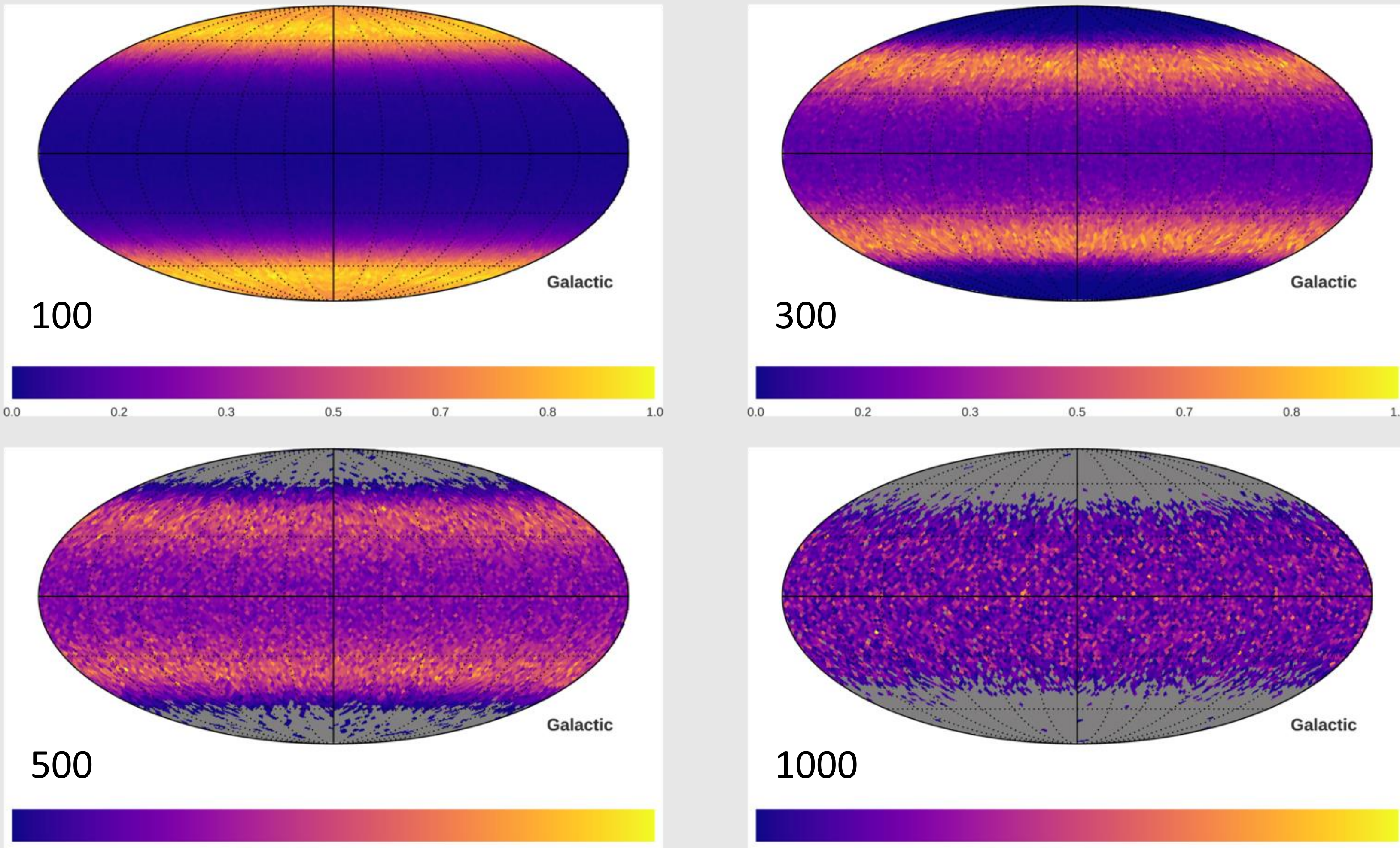

4 Arrival $\delta = 0.6, \epsilon = 0.1$; Wind

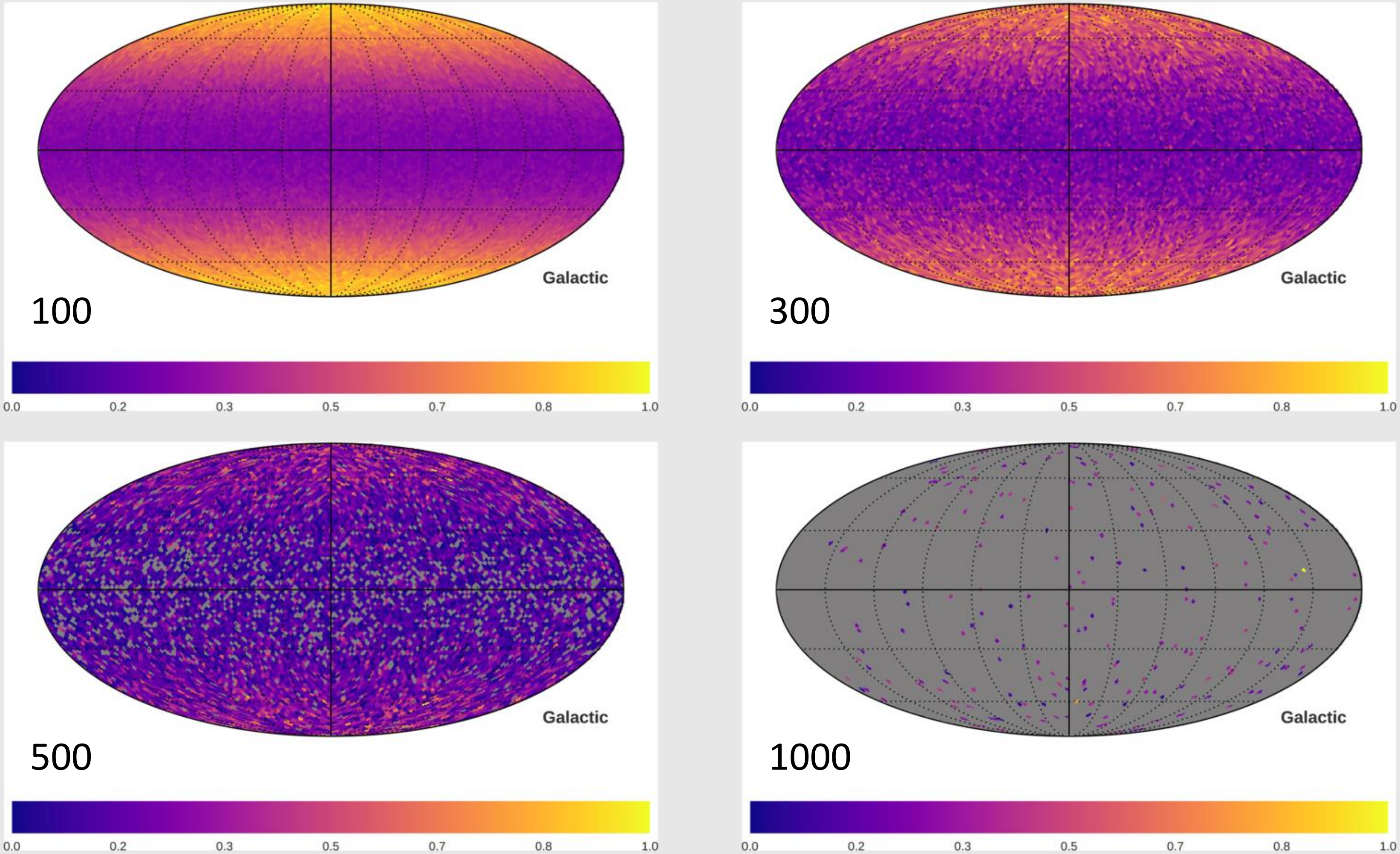

Extension

Outlook

Use the local turbulence ratio η with: $\eta = \frac{b_0^2}{b_0^2 + B_0^2}$ to calculate diffusion tensor.

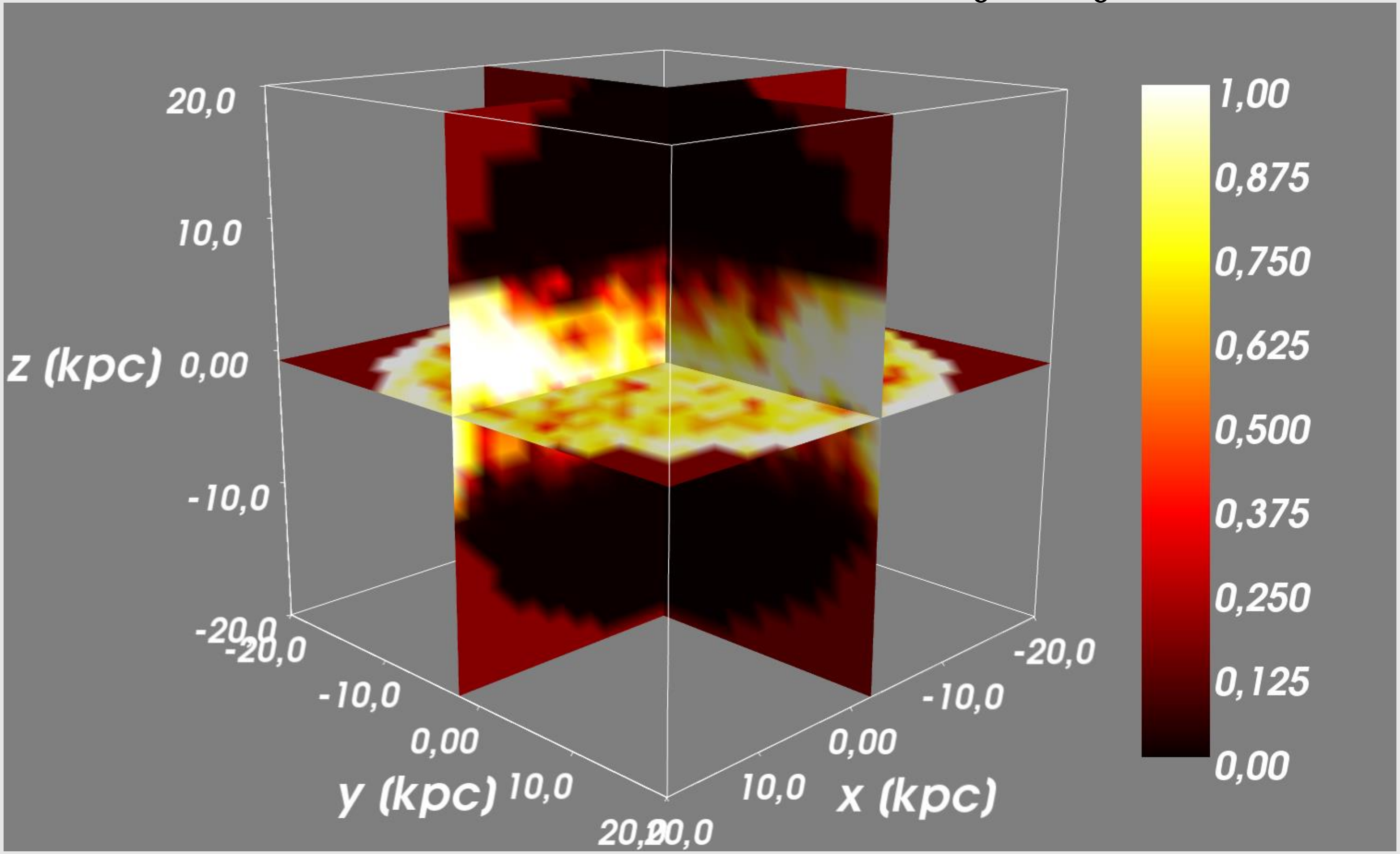

Fig 23: The turbulence ratio of the JF12 field.

Competitors

Comparison of Tools

Tab. 1: Popular Propagation Programs

Name	Propa-gation	Diffusion	Integration	Inter-action	Remarks	Cite
GALPROP	Trans. Equ.	Scalar	Grid (Crank Nicolson)	Yes	Quasi stand.	Strong et al. (2011)
DRAGON 2	Trans. Equ.	3dim anisotr.	Grid	Yes		Evoli et al. (2016)
PICARD	Trans. Equ.	3dim anisotr.	Grid	Yes	Dedicated stat. Solver	Kissmann et al. (2014)
CRPropa 3 (PropagationCK)	Equ. of Motion	No	Cash Karp	Partly	UHECR	Batista et al. (2016)
CRPropa 3.1 (DiffusionSDE)	**Trans. Equ.**	**3dim const. Eigenvalues**	**SDE adaptive**	**Partly**	**Arbitrary magn. field**	**Merten et al. (t.b.s.)**
	Trans. Equ.	Fully anisotropic	SDE Euler-Mayurama	No		Koppet al. (2011)